2021



UNIVERSITY OF BIRMINGHAM

THE RECYCLING OF LI-ION BATTERY ANODE MATERIAL USING SUPERCRITICAL SOLVENTS

FARADAY INSTITUTION RELIB PROJECT

SAMUEL SUDRON (MRES CHEMICAL ENG SCIENCE FR)

UNIVERSITY OF
BIRMINGHAM

University of Birmingham Research Archive

e-theses repository

This unpublished thesis/dissertation is copyright of the author and/or third parties. The intellectual property rights of the author or third parties in respect of this work are as defined by The Copyright Designs and Patents Act 1988 or as modified by any successor legislation.

Any use made of information contained in this thesis/dissertation must be in accordance with that legislation and must be properly acknowledged. Further distribution or reproduction in any format is prohibited without the permission of the copyright holder.

Declaration

I declare that the research conducted within this report was my own with help from the acknowledged; Luke Sweeney, Guozhan Jiang and Gary Leeke. This research has not been submitted in whole or part. Except where stated otherwise in either acknowledgement or reference.

Acknowledgements

I would like to express my very great appreciation to Gary Leeke for introducing me to this research, with his advice and knowledge of the field he was able to advise me throughout the project.

I would like to offer my special thanks to Guozhan Jiang for introducing me to the lab and helping throughout my research.

Advice given by Richard Greenwood has been a great help in joining this research team at the University of Birmingham.

Assistance provided by Luke Sweeney was greatly appreciated.

The Faraday Institution for giving a platform for the research on Li-Ion batteries to take place.

Table of Contents

Declaration 1

Acknowledgements 2

Figures 5

Tables 8

1 Abstract 9

2 Introduction 10

3 Literature Review 12

3.1 Lithium-Ion Batteries 12

3.2 Recycling of Batteries 15

3.2.1 Collection and Demand 15

3.2.2 Pyrolysis 16

3.2.3 Black Mass Production 17

3.2.4 Hydrometallurgical Processes 17

3.3 Supercritical Fluids 18

3.4 Graphite and Graphene 21

4 Materials and Methods 22

4.1 Materials 22

4.2 Supercritical Separation 22

4.3 Solid and Liquids Rotary Evaporation Separation 24

4.4 Solid and Liquids Filter Separation 25

4.5 Light Microscopy 27

4.6 Thermogravimetric Analysis 27

4.7 Infrared Spectroscopy (IR) 27

4.8 Scanning Electron Microscopy (SEM) 28

4.9 Graphene Production using Ultrasound 28

4.10 Graphene Production Rapid Pressure Release 29

4.11 Tunnelling Electron Microscopy (TEM) 30

5 Results and Discussion 31
5.1 Supercritical Separation 31
5.2 Light Microscopy 37
5.3 Thermogravimetric and Infra-red 41
5.4 Scanning Electron Microscopy (SEM) 46
5.4.1 SEM-EDX Data from Pure PVDF 46
5.4.2 SEM-EDX Data from Methanol Extracted PVDF 48
5.4.3 SEM-EDX Data from Ethanol Extracted PVDF 50
5.4.4 SEM-EDX Data from Acetone Extracted PVDF 52
5.4.5 SEM-EDX Data from Butanol Extracted PVDF 54
5.4.6 SEM-EDS Data from DCM Extracted PVDF 56
5.4.7 Overall SEM-EDS Data from Extracted PVDF 57
5.5 Tunnelling Electron Microscopy (TEM) 59
5.6 Continuous Separation and Upscaling 62
6 Conclusions and Further Work 67
6.1 Conclusion 67
6.2 Further Work 68
7 References 69

Figures

Figure 1 Structure of anode material with average mass percentages. 10
Figure 2 Structure of PVDF 11
Figure 3 General structure of a conventional Li-Ion Battery taken from (Bai et al., 2012). 13
Figure 4 Exponential Growth of Lithium-Ion batteries in the Global Market (Melin, 2020) 14
Figure 5 Phase Diagram for Ethanol showing the Critical Point 18
Figure 6 Schematic showing the effect of operational change to particle formation. Phase Diagram showing the change of pressure and temperature to form a fluid-solid (F-S) phase boundary or the possibility of a liquid-liquid phase boundary from a one phase solute-solution phase. (Yeo and Kiran, 2005) 19
Figure 7 Elimination reaction of PVDF with bases and the creation of HF (Marshall et al., 2021) 20
Figure 8 Showing the setup of supercritical separation; **1** Reactor Vessel **2** Reactor Head **3** Safety Pressure Valve **4** Thermal Probe **5** Pressure Reading and Probe **6** Gas Release Valve **7** Temperature Control Unit 23
Figure 9 Schematic of vessel used for supercritical separation 24
Figure 10 Rotary evaporator used for the separation of liquids and solids. 25
Figure 11 Vacuum pump (Stuart RE3022C) to remove liquid from solid particulate. 26
Figure 12 Drying oven (GPE E3) for PVDF and anode material. 26
Figure 13 Light Microscope used. 27
Figure 14 Setup of the high-pressure ultrasound vessel Used 28
Figure 15 Controller for the sonic probe (Sonic VCX 1500). 29
Figure 16 Flow diagram showing layout of graphene production vessel and gas container. 30
Figure 17 Image Showing Gas Containment Vessel for Rapid Pressure Release (Parr Instruments) 30
Figure 18 The products from the use of Water, Acetone, Ethanol, and Methanol supercritical extraction processes, respectively. 32
Figure 19 Image showing the Catalytic Cyclocondensation of Acetone to Isophorone (Ramanamurty and Salvapati, 1999) 33
Figure 20 Images showing pure PVDF (no processing) at zooms from x5 to x20. 37
Figure 21 Images of PVDF recovered after processing in Methanol at 91 bar and 250 °C and Ethanol at 69 bar and 250 °C 38
Figure 22 Images of PVDF recovered after processing in butanol at 56 bar at 290 °C and DCM at 67 bar at 250 °C 39

Figure 23 InfraRed spectrum of Pure PVDF (a) Composite membranes composite membranes blended with nano-crystalline cellulose (b) (Bai et al., 2012) 41
Figure 24 InfraRed Spectrum from Methanol extracted PVDF at 91 bar and 250 °C 42
Figure 25 InfraRed Spectrum from Methanol extracted PVDF at 91 bar and 250 °C 42
Figure 26 InfraRed Spectrum from Ethanol extracted PVDF at 69 bar and 250 °C 43
Figure 27 InfraRed Spectrum from Acetone extracted PVDF at 70 bar at 270 °C 43
Figure 28 InfraRed Spectrum from Butanol extracted PVDF at 56 bar at 290 °C 44
Figure 29 InfraRed Spectrum from DCM extracted PVDF at 67 bar at 250 °C 44
Figure 30 Image from Scanning Electron Microscope of Pure PVDF 46
Figure 31 Image from Scanning Electron Microscope of Pure PVDF with Elemental Analysis overpage 47
Figure 32 Images from Scanning Electron Microscope of Pure PVDF with individual element colour representations; Fluorine, Carbon, and Aluminium 47
Figure 33 Elemental Analysis of Pure PVDF 48
Figure 34 Image from Scanning Electron Microscope of Methanol Extracted PVDF at 91 bar and 250 °C 48
Figure 35 Image from Scanning Electron Microscope of Methanol Extracted PVDF at 91 bar and 250 °C with Elemental Analysis overpage 49
Figure 36 Images from Scanning Electron Microscope of Methanol Extracted PVDF at 91 bar and 250 °C with indivual element colour representations; Fluorine, Carbon, Oxygen, Phosphorus, Copper and Bromine 49
Figure 37 Data showing the Elemental Analysis of Methanol Extracted PVDF at 91 bar and 250 °C 50
Figure 38 Image from Scanning Electron Microscope of Ethanol Extracted PVDF at 69 bar and 250 °C 50
Figure 39 Image from Scanning Electron Microscope of Ethanol Extracted PVDF at 69 bar and 250 °C with Elemental Analysis overpage 51
Figure 40 Images from Scanning Electron Microscope of Ethanol Extracted PVDF at 69 bar and 250 °C with indivual element colour representations: Carbon, Fluorine, Silicon, Copper, Chlorine, Phosphorus. 51
Figure 41 Data showing the Elemental Analysis of Ethanol Extracted PVDF at 69 bar and 250 °C 52
Figure 42 Image from Scanning Electron Microscope of Acetone Extracted PVDF 52
Figure 43 Image from Scanning Electron Microscope of Acetone Extracted PVDF with Elemental Analysis overpage 53

Figure 44 Images from Scanning Electron Microscope of Acetone Extracted PVDF with indivual element colour representations, Fluorine, Carbon, Oxygen, Aluminium and Chlorine..... 53
Figure 45 Data showing the Elemental Analysis of Acetone Extracted PVDF..... 54
Figure 46 Image from Scanning Electron Microscope of Butanol Extracted PVDF at 56 bar at 290 °C 54
Figure 47 Images from Scanning Electron Microscope of Butanol Extracted PVDF at 56 bar at 290 °C with indivual element colour representations: Fluorine, Carbon, Aluminium, Silicon, Oxygen and Silicon..... 55
Figure 48 Data showing the Elemental Analysis of Butanol Extracted PVDF at 56 bar at 290 °C..... 55
Figure 49 Image from Scanning Electron Microscope of DCM Extracted PVDF at 67 bar at 250 °C 56
Figure 50 Images from Scanning Electron Microscope of DCM Extracted PVDF at 67 bar at 250 °C with indivual element colour representations: Carbon, Fluorine, Chlorine, Oxygen, Phosphorus and Aluminium..... 56
Figure 51 Data showing the Elemental Analysis of DCM Extracted PVDF at 67 bar at 250 °C 57
Figure 52 Images showing graphite produced from New Battery Grade Graphite processed using supercritical ethanol at 69 bar and 250 °C and fast pressure release..... 60
Figure 53 Images showing Graphene produced from End-of-Life Graphite processed using supercritical ethanol at 69 bar and 250 °C and fast pressure release..... 61
Figure 54 Flow Diagram for the Overall Continuous supercritical Extraction Process..... 63
Figure 55 Diagram Showing the Pipe Reactor that could be used to Extract PVDF. 64
Figure 56 Diagram showing the separation of the pipe reactor..... 65
Figure 57 The furnace that could be used for the Pipe Reactor (Carbolite Gero ELF 1100)..... 65

Tables

Table 1 Materials used with purity and supplier 22
Table 2 Conditions used in supercritical Separation 24
Table 3 Boiling point for solvents used 25
Table 4 Supercritical separation runs that were conducted, the solvents used and the initial and final masses. 31
Table 5 Acetone colour change tests with colour results. 33
Table 6 Average particle sizes from light microscopy. 40
Table 7 Overall Data for solvent SC extraction products for Infrared Analysis 45
Table 8 Overall SEM-EDS Data from Extracted PVDF showing Elemental Atomic % 58

1 Abstract

This research looks at the use of supercritical solvents on the potential of recycling the anode material from electric vehicle batteries. The anode material is made up of 5 layers; graphite, polyvinylidene Fluoride (PVDF), Copper, another layer of PVDF and another layer of graphite. This research looks at separating those layers using super critical fluid. The extraction of PVDF from between the copper and graphite, within the anode material, was done using a variety of solvents at supercritical conditions within a high-pressure vessel. The solvents used were acetone, methanol, ethanol, propanol, butanol, and dichloromethane (DCM). Acetone at these supercritical conditions self-reacted to produce iso-phorone. This caused the liquid to turn yellow due to the dissolved orange wax (iso-phorone). The alcohols all extracted the PVDF, this was tested using XRF, TGIR, Light Microscopy and SEM. A pattern was discovered that as the alcohol molecules C-number increased, so did the size of the PVDF particles and decreased the oxygen contaminant from 15% using methanol to 2% with butanol. This was concluded to be due to a decreased amount of depolymerisation taking place. The DCM produced a laminated PVDF product but included a graphite contaminate. Particles of PVDF being present due to it becoming dissolved in the solution at supercritical conditions and then precipitating during the cooling period of the vessel outside of the anode material.

Graphene was also produced using Supercritical fluids in a larger vessel with the help of a quick pressure release system. Graphene was produced using new and end-of-life graphite. Better results were found using end-of-life graphite, possibly due to the intermolecular forces becoming weakened over battery use. This may also produce a thinner and increase concentration of graphene. The use of ultra-sonic probe was inconclusive, further tests are required. Using this experimentation, a design for a continuous PVDF recovery was conceptualised for upscaled recycling in the future.

2 Introduction

The project was formed as part of the ReLiB project under the funding of the Faraday Institution. The ReLiB project stands for the Recycling of Lithium-Ion Batteries and is looking to produce the next generation of recycling procedures for recycling electric vehicle batteries. Part of this was looking into the use of Supercritical fluids to separate components from lithium-ion batteries. This small group of researchers was led by Prof Gary Leeke. With this research project looking into the use of supercritical fluids (SF) on the recycling of the anode material from a first-generation lithium-ion battery. The use of SF hopefully means there would be less effect on the environment and the production of waste products. The SF method would be compared to the use of other methods for the ReLiB project such as the use of mineral acids in conjuncture with shredding to produce black mass to be sorted later, the use of organic solvents at regular pressures and temperatures and using bio-products to break down plastics in the anode material using microorganisms. To begin into the use of supercritical solvents such as acetone and water, while also testing other supercritical solvents to establish the use in the future. The first-generation anode material is made up of a graphite layer consisting of polyvinylidene difluoride (PVDF) binder then laminated copper followed by another layer of PVDF and graphite. The PVDF acts as a binding agent for the battery layers, this can be seen as The SF project hopes to remove both layers without producing HF with the overall goal to separate all layers into their pure components. Figure 1 shows the structure as a diagram.

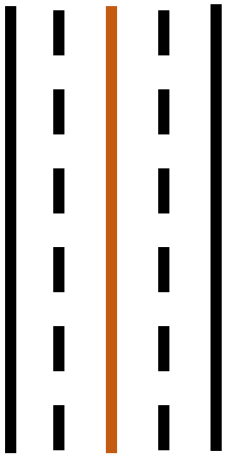


Diagram	Material	Average Mass %
	Graphite	52
	PVDF	45
	Copper	3

Figure 1 Structure of anode material with average mass percentages.

The products produced using different supercritical solvents will be analysed with an array of different analytical techniques, such as TGA and IR spectroscopy for the PVDF. With the recovered graphite with the hope to produce graphene. The upgrading of graphite to produce graphene has the potential to produce a product which in other circumstances would be more difficult without the weakening of the layers of graphite which has taken place due to the recurring electrical cycles through the battery. Using methods such as ultra-sonic waves and rapid pressure release while at supercritical conditions. All this moving away from the shredding of lithium-ion batteries to produce black mass, which consists of a fine black powder containing the metal oxide from the cathode and the graphite from the anode, so that more of the components and metal oxides can be recovered for future battery production.

The aim of this project is to investigate the recycling of Li-ion anode material by supercritical fluids and propose a method that allows continuous operation rather than batch to be attractive to the recycling industry. The separation of the PVDF, graphite and copper into different product streams is the end goal. This is so that supercritical fluids can be implemented into large industry production of lithium-ion battery components. With a focus on reducing waste products for recycling companies, while also making it as simple as possible so the implementation of these new methods is as easy as possible. This will be achieved with the use of testing the anode material within a high-pressure vessel and a selection of different organic solvents. They will be brought to supercritical conditions to hopefully separate the raw components. One of the big concerns of this method is the potential to produce HF from the degradation of PVDF and how this can be prevented from being produced. The structure of PVDF can be seen in Figure 1. This project incorporates the overall goals of the ReLiB project which is to set up designs for the recycling of electric vehicle batteries on a larger scale, moving away from the current method of shredding to black mass (powdered metal oxide and graphite).

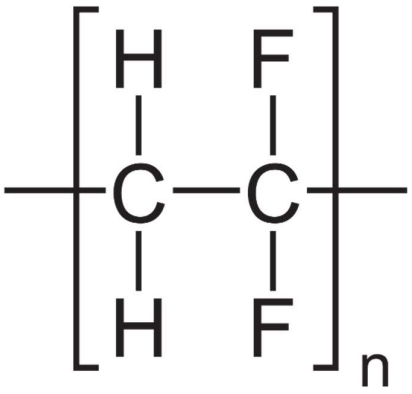


Figure 2 Structure of PVDF.

3 Literature Review

3.1 Lithium-Ion Batteries

This generation of lithium-ion batteries (LiBs) were first started to be developed in the 1990s, to be used on small electronics such as mobile phones laptops and tablets (Melin, 2020). This technology started to be used in vehicles around 2010 with this there was a rapid development of batteries meaning the production became more efficient leading to more research being conducted in the field of lithium-ion batteries (Melin, 2020). Rechargeable batteries have and can be used for energy storage in a more efficient manner than was previously available (Melin, 2020).

As the demand for lithium-ion batteries in both electric vehicles and portable electronic devices increases the improvements in research going into lithium-ion batteries will continue to increase. This is based on the historical evidence of new battery technology that has occurred in the past. There has never been quite an exponential growth in demand and research for a particular power source before this point. The use of lithium-ion batteries in practically every electronic device and upcoming vehicles due to CO_2 reduction laws coming into place, but due to the electricity source being primarily from a CO_2 producing source, this is not a fix. Many of the ways to characterise what occurs to the electrochemical performance while keeping the safety and efficiency of the battery consistent. With the overall goal to increase performance energy density longer lifespan and affordability of the batteries in the future, this can only occur with higher demand and the overall lead to further research (Tarascon and Armand, 2001).

A lithium-ion battery consists of an anode, an electrolyte, and the cathode. The cathode consists of a metal oxide structure which will help to hold the lithium ions while the battery is charged. The metal used in this oxide structure depends on the battery when it was developed and what generation it consists of (Duleep *et al.*, 2011). The metal oxide is bound to an aluminium current collector using mainly plastics to bond these two layers together. The electrolyte aids with the transportation of lithium ions from the anode to the cathode and back with a separator so that other molecules in the battery are unable to cross. The electrolyte consists of different cycling hydrocarbons to either form a gel or liquid-based electrolyte. The anode consists of a graphite layer where the lithium ions are held so that a charge can move from one side of the battery to the other. At the anode side of the battery there is a copper current collector, much like the cathode side of the battery there is a plastic binder which helps to keep the copper attached to the graphite carbon. The movement of lithium ions from one side of the battery to the other is what can produce an electric current for electrical storage (Nitta *et al.*, 2015).

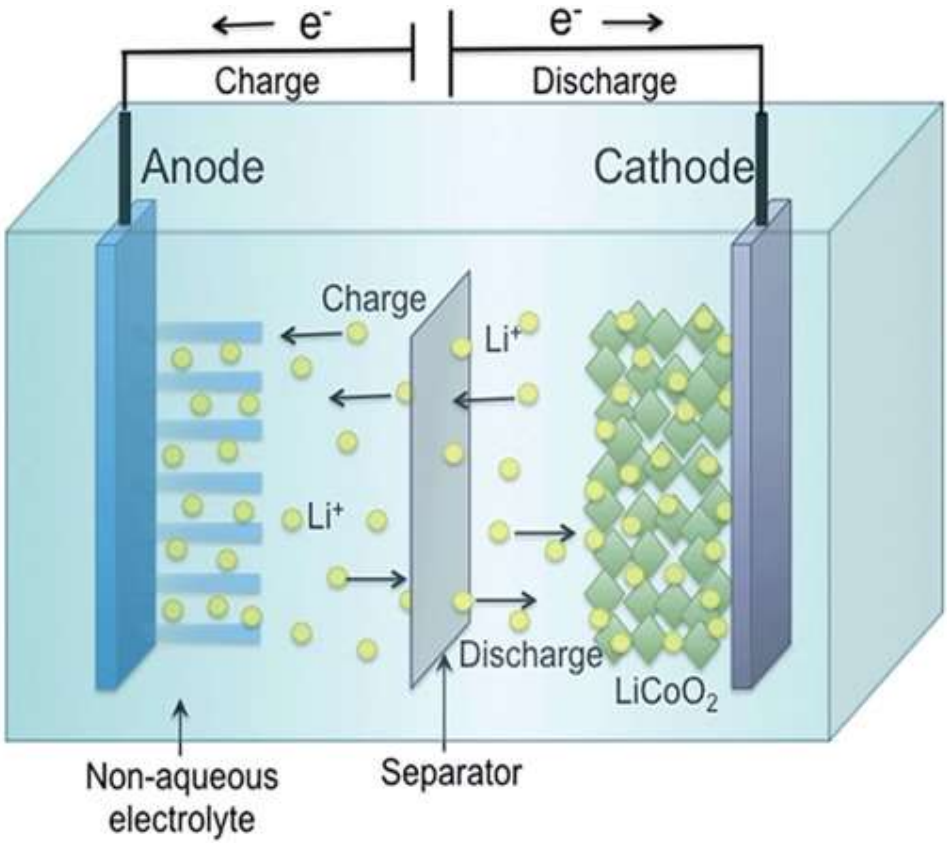


Figure 3 General structure of a conventional Li-Ion Battery taken from (Bai *et al.*, 2012).

Through multiple charges and discharges deterioration can occur which is why lithium-ion batteries will fall out of service. This can occur for a multitude of reasons. The binder between either the anode or cathode metal or current collector can decompose reducing the efficiency of the current collecting. The copper and aluminium current collectors can begin to corrode or dislocate and move into the battery structure, reducing the overall efficiency of the battery. The layers of graphite through multiple charges and discharges of lithium ions can break down producing movement between the layers reducing the overall space in which the lithium can take up, reducing the overall charge capacity. The separator used to keep other molecules in the battery from moving from the cathode to the anode can break down, allowing the movement of metal oxide molecules to become attached to the graphite structure which can cause a short circuit within the battery. With the breakdown of the metal oxide this will also reduce the overall charging capacity of the lithium ion battery (Bruce et al 2008).

As discussed before lithium batteries are experiencing an exponential requirement throughout the electronic and electric vehicle world, this can be seen as Figure 3. With a look into the potential of using higher capacity and longer life lithium-ion batteries within the renewable energy sector and storage. This requirement for large energy storage rather than more practical and lightweight storage

there has been required in the past opens a new avenue which there is hope this will achieve technological jumps in energy and power storage. The scaling up of lithium battery technology could be the next step into a greener future (Scrosati and Garche, 2010).

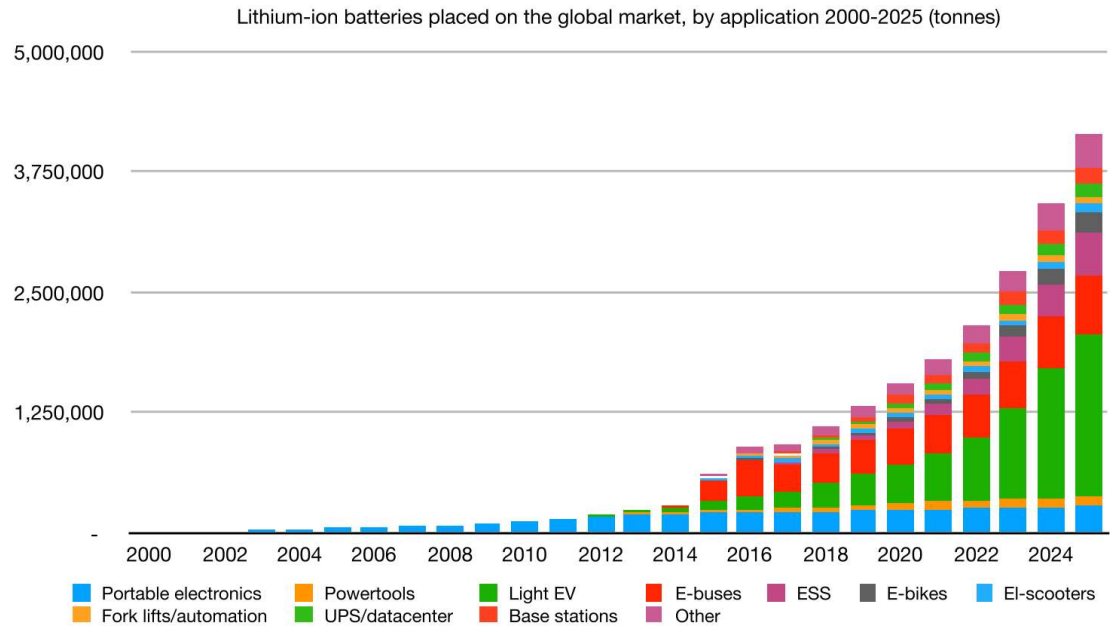


Figure 4 Exponential Growth of Lithium-Ion batteries in the Global Market (Melin, 2020)

Most renewable energy production varying in the amount of electricity they can produce throughout the year and the need for energy storage throughout the grid has been increasing in the past years with the government looking to a greener future. This has been used in the past with energy production such as hydroelectricity but with the use of lithium-ion batteries this could reduce the cost and increase the grids storage to a new level, removing one of the largest disadvantages to renewable technology. Researchers are hoping that this will be the boost renewable energy needs for more development to be established (Dunn, Kamath and Tarascon, 2011).

As laid out lithium-ion batteries may be rechargeable, but they do not have an unlimited life, with the lifespan of most first and second-generation lithium-ion batteries living around 10 years in electric vehicles and substantially less in portable and handheld electronic devices due to the increased need to recharge (Kang et al 2013). There has been an increase in research and development into the increased energy density and product life but the batteries that have already been introduced into the market are being discarded without being recycled. The metal content in each of the lithium-ion batteries has now been classified under US law as a hazardous material due to the excess levels of lead, cobalt, copper, and nickel within the batteries. These environmental impacts that could damage the ecosystem and human toxicity levels if it were to spread into the water table (Kang et al 2013).

With these findings in 2013 by the American Chemical Society there has been a new governmental policy (Kang et al 2013) in the increased research into recovery recycling and reuse of lithium batteries and their materials to reduce any further damage due to the toxicity levels of lithium ion batteries (Kang et al 2013).

Looking further into the future the application of ambient temperature sodium ion batteries is being developed by looking at the battery component materials for the possibility of producing a battery that could be used for large-scale grid storage at a lower cost than that of lithium-ion batteries (Zubi *et al.*, 2018). A material such as sodium the abundance of this material would mean that development could take place anywhere in the world with a reduction of mining affecting the environment and cost. The increased energy density that engineering models are producing show that it would completely replace that of lithium-ion batteries in the future (Zubi *et al.*, 2018). Due to sodium ions being available throughout the world research and development of ambient temperature sodium are batteries is quickly expanding so that these new batteries can be produced without relying on lithium in the Chinese market. Engineering advances show that this could be the potential low-cost long life future for grid storage (Slater *et al.*, 2013).

3.2 Recycling of Batteries

Reduce, reuse, recycle is the common phrase said by many to reduce the impact we are having with the use of materials on the environment. As a country recycling has been implemented into everyone's lives. To recycle or not to recycle that is the question. The idea to reduce needs to be explored, to reduce the number of materials that are being used in the first place so that we do not have shortages in the future (Song *et al.*, 2012). This needs to be implemented by large controlling companies and government bodies so that there is not as much waste. The idea to reuse in terms of batteries is being researched and used by large recycling companies such as Urecycle (Gaines, 2012). This is evaluating the effectiveness of the battery from old cars to be used in less strenuous environments. Such as using in the power storage for renewable power sources (Harper *et al.*, 2019).

3.2.1 Collection and Demand

There is a worldwide demand for the raw materials needed to make an increasing number of Li-ion batteries. With shortages worldwide of various materials there is a push to prevent the future shortages of these metals and oxides. The recycling of Li-Ion batteries is focused upon the recycling of electric vehicle batteries, rather than small appliance batteries. This is due to the overwhelming mass difference of the two sources. The research into this degree of recycling is also very limited, with most of the research taking place in China, Japan, and USA (Chen *et al.*, 2019). Due to lack of production

and recycling of LiBs in the UK until recently, this research field is still being explored. The methods that are being developed are to produce more efficient and cost-effective methods than pyrometallurgical procedures.

Not only the methods of recycling but also the collection of the batteries. Metal scrap recyclers need to be educated in new methods of separating, removing, and storing batteries. This is so to create an efficient supply chain of materials to the correct companies for reuse or recycle. The Li-ion market is still growing exponentially, so if recycling is to keep up, with electric vehicle batteries lasting approximately 10 years, research needs to increase at the same pace. The recycling facilities will need to continuously increase with production to recover these much-needed materials. Batteries are being manufactured by different companies all over the world, using different metal oxides, configurations, and assembly. Meaning that producing a universal recycling method is that much more difficult. Batteries are also being produced for industrial with around double the cycle life than that of the portable batteries for smaller devices. In just five years of production, the tonnage of industrial batteries has overtaken portable batteries. The lifetime of these batteries should be around 10 years but there seems to be an average collection time of 6 years. Which is why reuse of these batteries needs to be worked on as hard as recycling, as its unfeasible to recycle that many batteries in such a short amount of time. Recycling in Europe very limited, this can be explained by the lack of research and the lack of a supply of end-of-life lithium-ion batteries being collected compared to that of China or South Korea (Mossali *et al.*, 2020). Due to a lack of recycling, we also have a lack of raw materials to manufacture new Li-ion batteries within Europe and the UK. With China also using hydrometallurgical procedures, they can achieve much higher yields than in Europe using pyrometallurgical and mechanical methods. This needs to change if Europe is to become independent from the China for battery production (Fan *et al.*, 2020). A stable supply chain needs to be developed from end-of-life to new with the use of recycling and reuse. The development of more efficient, cost-effective and profitable techniques needs to be at the forefront of research (Melin, 2020).

3.2.2 Pyrolysis

Pre-treatment is often overlooked when thinking about the recycling of batteries. There being assorted designs for Li-ion batteries, so to produce a uniform recycling process the use of pre-treatment will need to be proven. This is less needed if a more mechanically driven process is to be used. Demonstrating the use of such dismantling or a small amount of crushing before using a hydrometallurgical process has led to increased yields in required products. Pyrometallurgical techniques result in the use of high temperatures increasing from 300^{o}C to around 700^{o}C for the pyrolysis of products (Huang *et al.*, 2018). Gases can be retrieved at different temperatures for various products. Leading to the retrieval of large organic compounds. The most important from this

technique is for the removal of copper, cobalt, nickel, and iron forming alloys, with lithium, aluminium, silicon, and calcium forming oxides. This process uses massive energy intensive and expensive to run, with a low recover rate it is important to move away from this type of process (Huang *et al.*, 2018).

Most industrial recycling processes investigates the use of pyrometallurgical processes which are expensive and highly energy intensive. Funded projects, such as the ReLiB project, investigate the use of more energy efficient processes ways to remove the use of elevated temperature processes and using more mechanically driven methods. The use of these mechanical processes and upscaling laboratory research (Diekmann *et al.*, 2017).

3.2.3 Black Mass Production

Whole battery modules are crushed using mechanical action with a shredder, this removes a portion of the wanted product or black mass. Black mass is the name for the powdered product (less than 250 micrometres). The black mass has the metal oxide from the cathode and the graphite from the anode, along with the binding agent (PVDF). With more mechanical action with the use of a balling mill an overall yield of material to around 75%. Drying of the products are needed to remove the electrolyte so not to create an impure black mass. This process is safe and lacks the use of environmentally harmful chemicals to produce dry products ready for reprocessing (Yun *et al.*, 2018). This process is a dry, quick, and cheap method that can be implemented into recycling centres around the world. This method is being moved away from due to its lack of profitable products and reduced recycling rate. This is still better than not recycling at all.

3.2.4 Hydrometallurgical Processes

The current methods that are being explored for upsizing are focusing on the treatment of black mass to extract the precious metals such as Nickel and Cobalt. Due to a lack of effective and quick preparation techniques of batteries without producing black mass, it is hard to have anode or cathode material separated from the rest of the battery. Working on the idea that these preparation techniques are currently being worked on to produce a robotic solution that could breakdown a batterie to cell level, hydrometallurgical processes are being designed to effectively retrieve raw materials for new battery production that could be conducted within the UK or home country to reduce carbon emissions of transport and mining. One material which is overlooked is the battery grade graphite that is retrievable from the anode. To be able to retrieve this so that it is uncontaminated by binder or copper is why this research was started.

3.3 Supercritical Fluids

Supercritical fluids are a phase of matter a chemical when it goes above the Tc and Pc. This can be seen in Figure 4 below. A supercritical fluid has the properties of a liquid and a gas. It can dissolve materials like a liquid and effuse through porous solids like a gas.

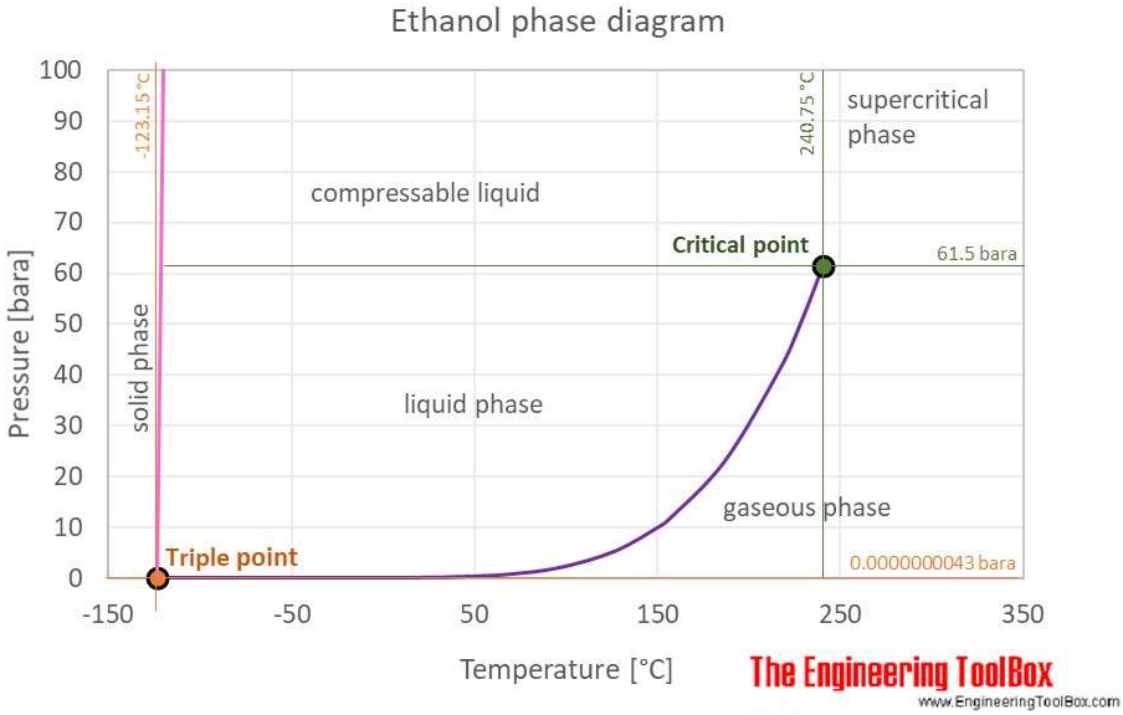


Figure 5 Phase Diagram for Ethanol showing the Critical Point

Another use of supercritical organic solvents investigates the use of methanol at a supercritical temperature of 300°C and pressure. This research is based on the idea to disassemble lignin from biomass into processible units. The experiment utilises a Cu doped porous catalyst at supercritical temperatures. The methanol acts as a hydrogen doner for the lignin causing the hydrogenolysis of the phenyl ether bonds causing the deconstruction of the lignin. This technique has been repeated, using different catalysts and different solvents all at supercritical conditions and using a catalyst. The techniques use long processing times of around 6 hours to completely break down the lignin into its deconstructed parts. The use of the catalyst was integral to the reaction as the temperature that would be required would cause the products to deform and be less useful for future processing. The products were analysed using NMR spectroscopy and GCMS. The use of ethanol instead of methanol resulted in a higher reaction time and pressure being needed. This research produces products that could be used as renewable carbon replacements for chemical and material applications. (Barta *et al.*, 2010)(Huang *et al.*, 2014)(Warner *et al.*, 2014)

Carbon-fibre-reinforced plastic (CFRP) is a difficult material to recycle due to its nano structure. The plastics being used in this way are often thermosetting plastics, adding to the difficulty of the recycling. In (Okajima and Sako, 2019) they use the methods of supercritical solvents. Acetone is the solvent they have chosen, and they heat it up to supercritical conditions of 350C and 14 MPa. The products were examined after different reaction times. The product production efficiency increased to 95.6% after 60 mins but after this time the reaction caused the product to carbonize. The conditions of the supercritical acetone caused the plastic to shrink away from the carbon fibre and dissolve into the acetone. (Okajima and Sako, 2019)

The methodology of using rapid expansion of supercritical solutions (RESS) of polymers is used when a polymer wont dissolve under standard conditions. The polymer and chosen supercritical solvent while at supercritical conditions will form a 1-phase matrix where the polymer will become dissolved within the solvent. Once the temperature or pressure drops causing the solution to drop out of supercritical conditions, a 2-phase solution is formed where the polymer forms solid particles within the solution. This can be improved upon by using rapid expansion with the use of a nozzle (Yeo and Kiran, 2005). This can be seen in Figure 6 below.

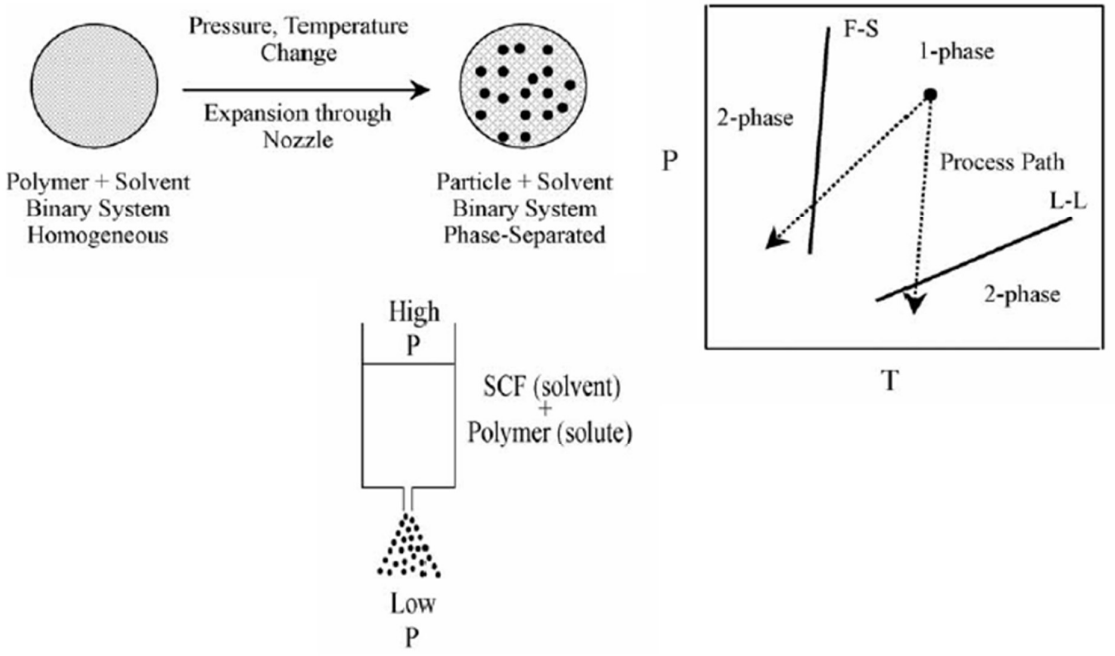


Figure 6 Schematic showing the effect of operational change to particle formation. Phase Diagram showing the change of pressure and temperature to form a fluid-solid (F-S) phase boundary or the possibility of a liquid-liquid phase boundary from a one phase solute-solution phase. (Yeo and Kiran, 2005)

Research has been conducted on the recycling of Polyetheretherketone (PEEK) composite material a plastic carbon fibre composite that only thermally decomposes at 703K. This study looks at the use of a supercritical fluid of ethanol and water to help with the degradation process. The use of a caesium carbonate as a catalyst is also used. This takes place in a high-pressure bomb reactor. The result being that the decomposition can take place at 623K rather than 703K. The separation of the carbon fibre strands from the plastic material at lower temperatures than that of thermal decomposition(Dandy *et al.*, 2015). The use of this method brings up the idea of removing PVDF from the graphite layers without destroying the PVDF, allowing for recovery of the plastic and graphite in its pure forms.

Overall PVDF is a stable plastic under high temperature and chemical, this is down to the strength of the C-F bond within its structure. Although as it is only containing one of these bonds in its monomer it does mean that it can still react under the right conditions. Thermally at atmospheric pressure and around 440 °C PVDF begins to breakdown thermally into hydrogen fluoride (HF) and smaller fluorinated hydrocarbons. Meaning that under higher pressures the PVDF could also breakdown at far lower temperatures. PVDF also has very strong chemical stability, acids have little to no effect on causing a reaction of PVDF. Studies have been conducted and low PH levels with hydrochloric acid, humic acid and sulphuric acid have no effect on PVDF. However, when exposed to strong alkaline conditions, the reaction is very similar to that of thermal degradation, HF is produced and C=C bonds are formed. If there are enough OH radicals these can react creating C-OH bonds within the structure of the PVDF and bridging between polymers. (Marshall *et al.*, 2021)

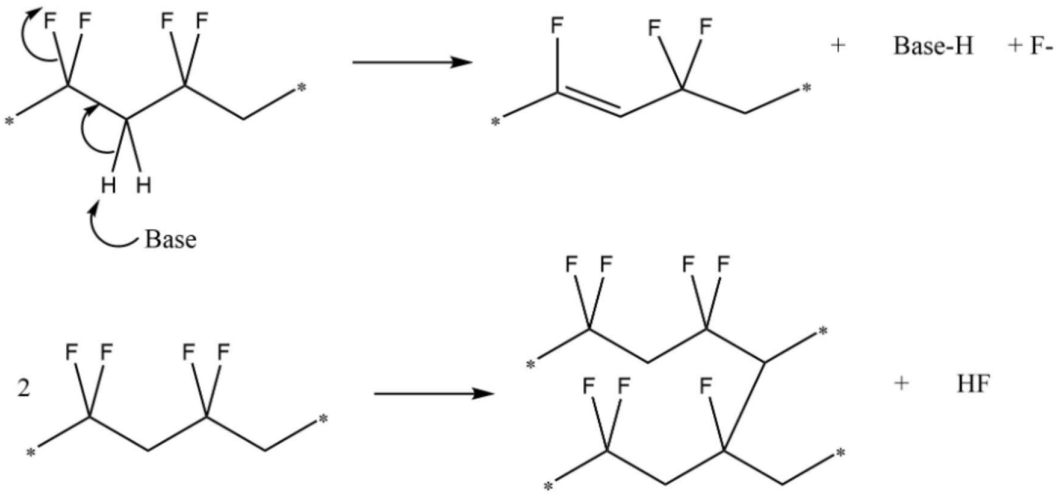


Figure 7 Elimination reaction of PVDF with bases and the creation of HF (Marshall et al.*, 2021)*

3.4 Graphite and Graphene

The recycling of graphite in the anode material of lithium-ion batteries forms an opportunity that is yet to be fully researched into its possibilities. Graphite that is used in lithium-ion batteries is of an extremely high-grade source. With the world trying to move away from the reliability on mining, graphite/graphene recycling needs to be explored more in depth. There is a growing need for flake graphite not just for commercial lithium-ion batteries, but to also generate a source for graphite within Europe and the UK (Moradi and Botte, 2016). For the possibility of recycling graphite, it requires methods that are not currently being used today. Methods such as pyrometallurgical are too destructive, the requirements for pre-treating such as disassembly into the factories individual parts separating the anode and cathode may be required. This will mean the research into dismantlement, through robotic means so to decrease health and safety risks (Moradi and Botte, 2016).

With recent research looking into the possibilities of the products graphene could produce. Physical and chemical properties that graphene possesses has contributed too many publications and the increase of research within the area (Zhu *et al.*, 2010). Within the area of lithium-ion batteries, graphene could be the way forward into producing the next generation of power storage. Within the production of graphene, graphene oxide seems to have a more stable and more reliable storage state. The production of graphene has been linked to the recycling of anode graphite material. With batteries undergoing multiple repeated charge and discharge cycles, this can lead to the weakening of the internal layer forces of the graphite structure. Experiments show that using some occasion the anode graphite produces 3 to 10 times higher yield of graphene than that of natural graphite (Chen *et al.*, 2017). What is also shown is that the lay account of the graphene layers be used from the battery source are of 1 to 4 graphene sheet thick (Chen *et al.*, 2017).

Supercritical fluids can be used to stabilise nanoparticles while also reducing metal oxides of nanoparticles, mostly focusing on organic solvents such as methanol and ethanol (Kim *et al.*, 2008). With graphene research accelerating the idea of stabilising nanoparticles fluids has been experimented with positive results (Seo *et al.*, 2013). The use of supercritical alcohols on graphene oxide has resulted in the production of graphene nano sheets with a high electronic conductivity and high lithium storage capacity stops this has been tested on penny battery anode material (Budi Nursanto *et al.*, 2011). The use of supercritical ethanol from the production of graphene is also being investigated using some occasion and rapid release of pressures to produce single too few layers graphene. This has been characterised using scanning electron microscopy and transmission electron microscopy (Hadi *et al.*, 2016).

4 Materials and Methods

Polyvinylidene difluoride (PVDF) has the potential at experimental conditions to produce hydrogen fluoride (HF) (Marshall *et al.*, 2021). This limited the use of multiple analysis techniques due to HFs destructive properties. Chemicals used in experiments were used as received.

4.1 Materials

Table 1 Materials used with purity and supplier

Chemical	Purity	Supplier	Chemical Formula	Molecular Weight	Atmospheric Boiling Point (°C)	SC Temperature (°C)	SC Pressure (bar)
Acetone	99.8%	FisherSci	$(CH_3)_2CO$	58.08	56.0	235	47
Methanol	99.8%	FisherSci	CH_3OH	32.04	64.7	240	82
Ethanol	99.8%	FisherSci	C_2H_5OH	46.07	78.4	241	63
Propan-1-ol	99.8%	FisherSci	C_3H_7OH	60.09	97.0	263	52
Butan-1-ol	99.8%	FisherSci	C_4H_9OH	74.12	117.7	288	50
Dichloromethane (DCM)	99.8%	FisherSci	CH_2Cl_2	84.93	39.6	237	61
Water	~	Tap, undistilled	H_2O	18.01	100	374	221
Anode	~	Nissan Leaf	~	~	~	~	~
Graphite	~	Battery grade, pre-use	~	~	~	~	~

4.2 Supercritical Separation

Through this process the goal is to extract the PVDF from between the copper and graphite using a supercritical fluid. Using a 500 mL high pressure reactor chamber (Parr Series 4760) with a 300-bar seal limit, with a 250-bar safety valve, motor powered rotational rotor, water cooling system for motor, Parr electronic temperature control and pressure display. 150 mL of solvent fluid was added to each run with the addition of approximately 1.5 g of anode material (Nissan Leaf), this was added to the pressure vessel. The vessel would then be sealed in place using screws and clamp as seen in Figure 8. The cooling system for the motor would then be activated to keep it under 40°C so not that it's not damaged by the high heat. The temperature would then be set to around 10°C above the supercritical temperature of the solvent fluid. The vessel would then be allowed time to heat up to the working temperature, taking around 1 hour for the heater to get the fluid up to conditions. The pressure would then be checked to make sure that it had reached supercritical conditions. The

separation conditions are found below in Table 2 Conditions used in supercritical Separation. The solvent would then be left at these conditions for 15 minutes, to allow time for the binder to be dissolved. The heater would then be removed from the around the vessel and would be allowed to cool down. This would take at least 5 hours to reach room conditions. Once back to room temperature the vessel would then be opened, and its contents removed and then cleaned for the next run.

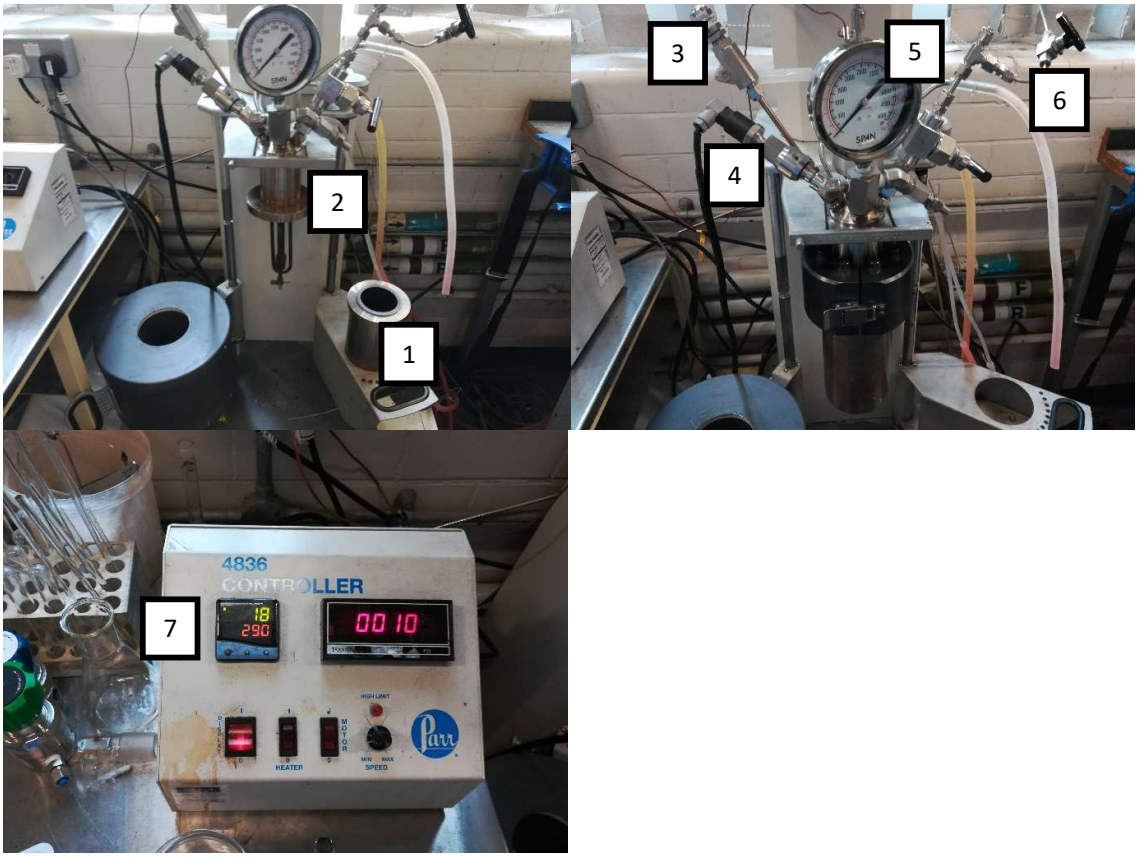


*Figure 8 Showing the setup of supercritical separation; **1** Reactor Vessel **2** Reactor Head **3** Safety Pressure Valve **4** Thermal Probe **5** Pressure Reading and Probe **6** Gas Release Valve **7** Temperature Control Unit*

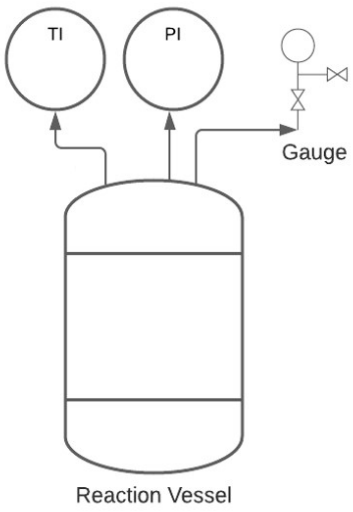


Figure 9 Schematic of vessel used for supercritical separation

The conditions in Table 2 were used so that both the temperature and pressure were higher than the required conditions for the fluids to become supercritical.

Table 2 Conditions used in supercritical Separation

Solvent	Critical Temperature (°C)	Critical Pressure (bar)	Experimental Temperature (°C)	Experimental Pressure (bar)
Water	374	221	375	230
Acetone	235	47	270	70
Methanol	240	82	250	91
Ethanol	241	63	250	69
Propanol	263	52	270	62
Butanol	288	50	290	56
DCM	237	61	250	67

4.3 Solid and Liquids Rotary Evaporation Separation

The rotary evaporator (SCILOGEX R100-S) was used to remove the initial large volumes of liquid that contained the PVDF and other solids. A water bath would be filled and heated to the evaporation temperature of the solvent, to gently heat the mixture within the flask. The glass flask shown in Figure 10 would then begin to spin to aid in evaporation. Cold water would travel through the twisted glass tubing to cause the solvent to condense into the other flask. This would continue until no more of the solvent was left. This was used for the colour acetone tests and to remove PVDF later described in the results. This was done to concentrate the material that was important to test, to allow for more reliable results.

Table 3 Boiling point for solvents used

Solvent (Test)	Evaporation Temperature (°C)
Water	100
Acetone	56
Methanol	65
Ethanol	78
Propanol	97
Butanol	118
DCM	40



Figure 10 Rotary evaporator used for the separation of liquids and solids.

4.4 Solid and Liquids Filter Separation

Vacuum filter separator was used after the rotary evaporator for the remaining solid material that was left after evaporation. The use of a vacuum pump (Stuart RE3022C), shown in Figure 11**,** and a ceramic filter to remove the PVDF from solvents. The ceramic filter was set up above glass flask attached to the vacuum pump, which helped with speeding up the separation. Once all the solvent had passed through the filter, filters were removed from the flask and left overnight in a drying oven (GPE E3), at 40 °C, so that the solid was completed dry as seen in Figure 12.



Figure 11 Vacuum pump (Stuart RE3022C) to remove liquid from solid particulate.



Figure 12 Drying oven (GPE E3) for PVDF and anode material.

4.5 Light Microscopy

Light Microscope (Zeiss Scope A1) was used to observe the morphology of the PVDF that was collected from the separation processes. The light microscope used a computer program so that pictures could be taken at x5, x10, x20 and x50 magnification, to allow for the full picture of the crystals to be shown. The dried material was not treated in any way before being observed.



Figure 13 Light Microscope used.

4.6 Thermogravimetric Analysis

Thermogravimetric analysis (TGA) was used to volatise the polymer using temperature to assess its degradation fingerprint against that of pure PVDF. Sample of 1-3g was loaded into a small ceramic container and is placed inside the machine. The temperature was then increased from room temperature to 300 ^{o}C. The mass of the sample was measured throughout as it's heated in N_2 gas. The gas produced was then put through Infrared Spectroscopy, so that the spectra of the lost material could be diagnosed by analysing its functional groups.

4.7 Infrared Spectroscopy (IR)

Samples of solid products loaded into the TGA were then fed into the Infra-Red Spectrophotometer. The infrared wavelength absorption generated a spectrum which could then be analysed to determine the functional groups in the gas phase molecules, measuring between 600 and 4000 cm^{-1}, over a period where the chemicals had been separated using TGA.

4.8 Scanning Electron Microscopy (SEM)

Due to COVID-19 regulations this analysis technique was carried out by personnel in the School of Chemistry at the University of Birmingham. Like Infrared spectroscopy solid samples collected from supercritical separation were observed under SEM to determine the crystal structure and elemental analysis using Energy Dispersive Spectroscopy (EDS). This was used to determine if the product contained PVDF.

4.9 Graphene Production using Ultrasound

Using a similar high-pressure vessel as used in supercritical separation, a 1 L vessel (Parr Series 4670) was used with a sonic probe instead of a mixer. 250 mL of ethanol was added with 1g of battery grade graphite. This is using a similar method to an experiment discussed previously by Kim et al., 2008. The vessel was then sealed using screws and clamp as seen in Figure 14**.** The sonic probe was then used for 20 min, 5 s on 5 s off in a cycle at 1500 Watt. Using the same temperature controller, the solution was brought up to supercritical conditions as seen in Table 2. Once at temperature the sonic probe was activated again for 20 min and with the same cycle. The vessel was then rapidly cooled by removing the vessel from the heater and plunged into cold tap water. It was held there until the temperature and pressure was back down to room temperature. This took approximately 10 min. The clamp was then removed, there was solid material floating on the top of the ethanol and this was removed first. The ethanol and suspended solid material were then removed and quickly added to a centrifuge, so to not let the solid material settle.

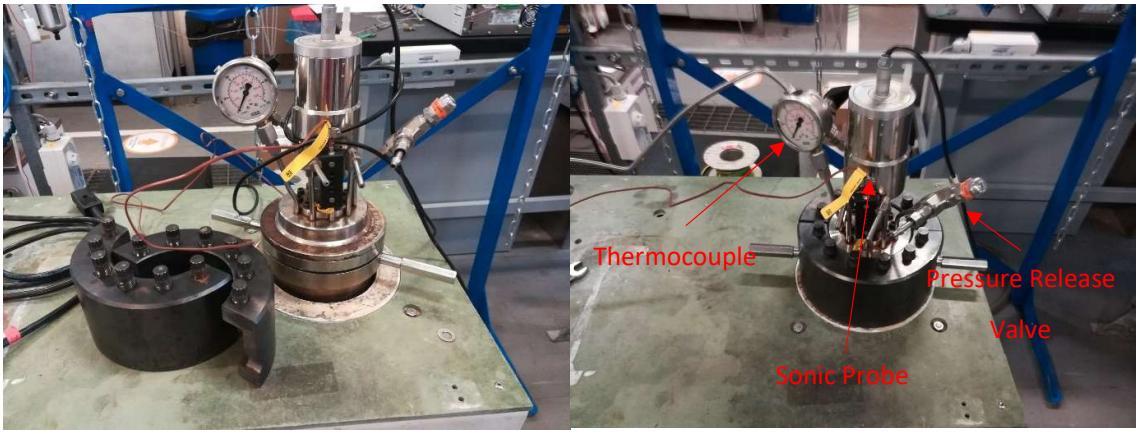


Figure 14 Setup of the high-pressure ultrasound vessel Used



Figure 15 Controller for the sonic probe (Sonic VCX 1500).

4.10 Graphene Production Rapid Pressure Release

The reason for this method is exploit the weakened Van der Waals forces. Using the same vessel as 4.8, 250 mL of ethanol was added with 1 g of battery grade graphite. The vessel was then sealed using screws and clamp as seen in Figure 14**.** The vessel was then attached with a gas containment vessel to the quick release valve at the top of the vessel as seen in Figure 15**.** The gas containment vessel as seen in Figure 17 was fitted with two valves either side so that the released material could be contained. Using ¼ inch piping the reactor and gas container were attached. Using the same temperature controller, the solution was brought up to supercritical conditions according to Table 2. Once at temperature the valve at the gas container was opened then the quick release valve was opened. Emptying the 1 L container in approximately 10 seconds. The supercritical fluid and suspended solid material were then forced into the container. The container valve was then closed followed by the quick release valve. The piping was then removed, and the gas vessel was rapidly cooled under a cold tap, taking around 5 minutes to cool down to room temperature. The liquid and suspended solids were then transferred to a centrifuge so to avoid sedimentation of the solid particles.

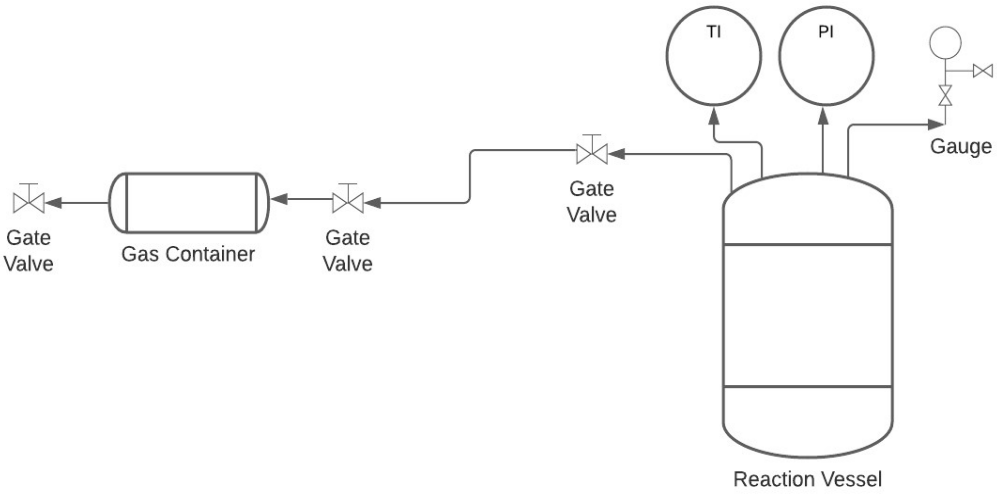


Figure 16 Flow diagram showing layout of graphene production vessel and gas container.

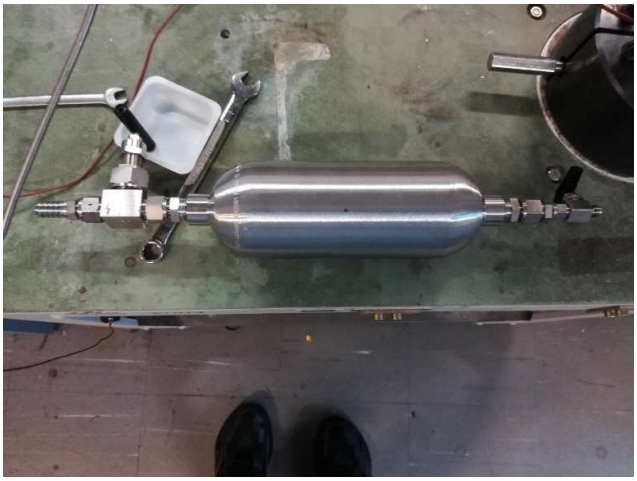


Figure 17 Image Showing Gas Containment Vessel for Rapid Pressure Release (Parr Instruments)

4.11 Tunnelling Electron Microscopy (TEM)

This is to determine if the rapid pressure release has produced graphene. Due to COVID-19 regulations this analysis technique was carried out by members of the School of Metallurgy and Materials. The solution was first processed using a centrifuge to increase the concentration of the nanoparticles so that the location of these particles could be located easier. Images were then taken at different levels of zoom so that the layers of the graphene could be observed.

5 Results and Discussion

5.1 Supercritical Separation

As explained in the method, the supercritical separation process used a high-pressure high-temperature vessel which held the anode material and the chosen solvent. The idea behind using this method is so that at these high pressure and temperatures the solvents would be able to dissolve the PVDF while at SC conditions. When the vessel is cooling and the solvent drops out of supercritical conditions, the PVDF would precipitate out of the solvent and out of the anode structure. This means that the PVDF would be recoverable, and the graphite could be removed uncontaminated by the PVDF binder agent. The first trial used water as solvent, water has a much higher supercritical point than the other solvents used which can be seen in Table 4, due to the hydrogen bonds of the molecule.

Table 4 shows all the supercritical separation experiments conducted and the conditions. The anode was weighed before and after to find the mass of PVDF that was extracted.

Table 4 Supercritical separation runs that were conducted, the solvents used and the initial and final masses.

Solvent (Test)	Temperature (°C)	Pressure (bar)	Anode Mass (g)	Mass After SC (g)	PVDF (g)	(3% of Mass) Appox Max PVDF(g)	Recovered PVDF(%)	Notes
Methanol (1)	250	91	1.6861	1.5191	0.0232	0.0506	46%	
Methanol (2)	250	91	1.8451	1.6716	0.0388	0.0554	70%	
Ethanol (1)	250	69	1.6447	1.4802				White substance left in suspenstion
Ethanol (2)	250	69	1.6521	1.4852				White substance left in suspenstion
Ethanol (3)	250	69	1.782	1.6216				White substance left in suspenstion
Ethanol (4)	250	69	2.1003	1.8986				White substance left in suspenstion
Ethanol (5)	250	69	1.7275	1.5642	0.0210	0.0518	41%	
Propanol (1)	270	62	1.7232	1.5284	0.0048	0.0517	9%	
Butanol (1)	290	56	1.9088	1.7408	0.0430	0.0573	75%	
Acetone (1)	270	70	1.7272	1.5134				Acetone has become yellow (isophorone). Boiling the acetone off created a orange wax.
Acetone (2)	270	70	1.658	1.4852				Same Yellow colour as before.
Acetone (3)	270	70	1.6162	1.4755	0.0190	0.0485	39%	
DCM (1)	250	67	1.8601	1.6628	0.0560	0.0558	100%	
Water (1)	375	230	1.6506	1.4957				Valve Burst due to high pressure. Graphite completely removed from Copper.
Water (2)	375	230	1.4232	1.2666				Graphite Removed from Copper

This meant that to increase the pressure to limiting points of the vessel and halt this in the first attempt because the safety release valve to burst under the high pressure. The vessel was allowed to cool and as it had reached supercritical conditions, and then we examined the effect on the anode material. The graphite and PVDF surrounding the copper of the anode were completely removed. The graphite was recoverable in large flakes, but the PVDF was not recoverable. The PVDF under such high pressure and temperature caused the structure to depolymerise. Once the new safety valve was installed with a higher safety pressure but still under the maximum pressure for the vessel, water was used again with the same result. PVDF was unable to be found even after evaporation of the water and the

graphite had no traces of plastic. Since the PVDF could not be found it is assumed that it was released when the safety valve burst. Due to this result, it was concluded the water would not be a suitable solvent for this process, PVDF being irretrievable, the graphite becoming damaged, and the much higher temperature and pressure required for the process, this can be seen in Figure 16.

Acetone was the next solvent to be tested under supercritical conditions the PVDF would be able to be removed without damaging the graphite or the copper. Using the same method as before but at different conditions it was found that the anode looked undamaged with the graphite still attached to the copper. Under further examination the graphite was easily removed from copper unlike unprocessed anode material. This was likely due to the PVDF becoming removed from between the copper and graphite making it easier to remove the graphite. But when the acetone was examined, it had turned yellow. It was first thought that the PVDF had caused the change in colour as seen in Figure 18, but there was also the possibility that this was a one-off, so the experiment was run again with the same conditions. The second run with acetone gave the exact same result so more tests had to be conducted. The acetone was first evaporated, and an orange wax was found.

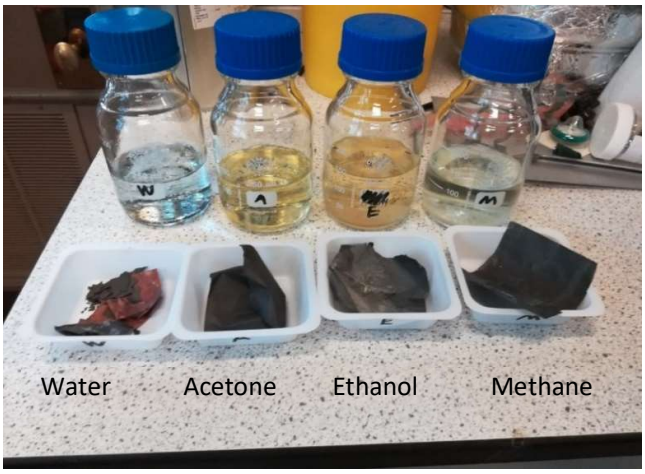


Figure 18 The products from the use of Water, Acetone, Ethanol, and Methanol supercritical extraction processes, respectively.

Table 5 shows the multiple tests were run, the first with just acetone, then acetone and graphite, then acetone and copper and finally with acetone and pure PVDF. From the results that this produced it was determined that the acetone was reacting to create a new molecule. The graphite and the copper acted as a catalyst to the reaction of the acetone as there was a deeper colour change and more wax like product produced.

Due to the colour of the acetone changing during separation runs, more experiments needed to be conducted to determine the origin of the colour change.

Table 5 Acetone colour change tests with colour results.

Acetone Tests	270 °C 70 bar

Solvent Mix	Colour
Pure Acetone	Light Yellow
Acetone + Graphite	Darker Yellow (Same Shade as with Anode)
Acetone + Copper	Darker Yellow (Same Shade as with Anode)
Acetone + PVDF	Light Yellow (Same as Pure Acetone)

Looking further into this it was found that the discolouration was most likely caused by a Catalytic Cyclocondensation reaction of Acetone to Isophorone as shown in Figure 19. Looking into the upscaling of this process for industry use it was likely that acetone could not be used due to this reaction.

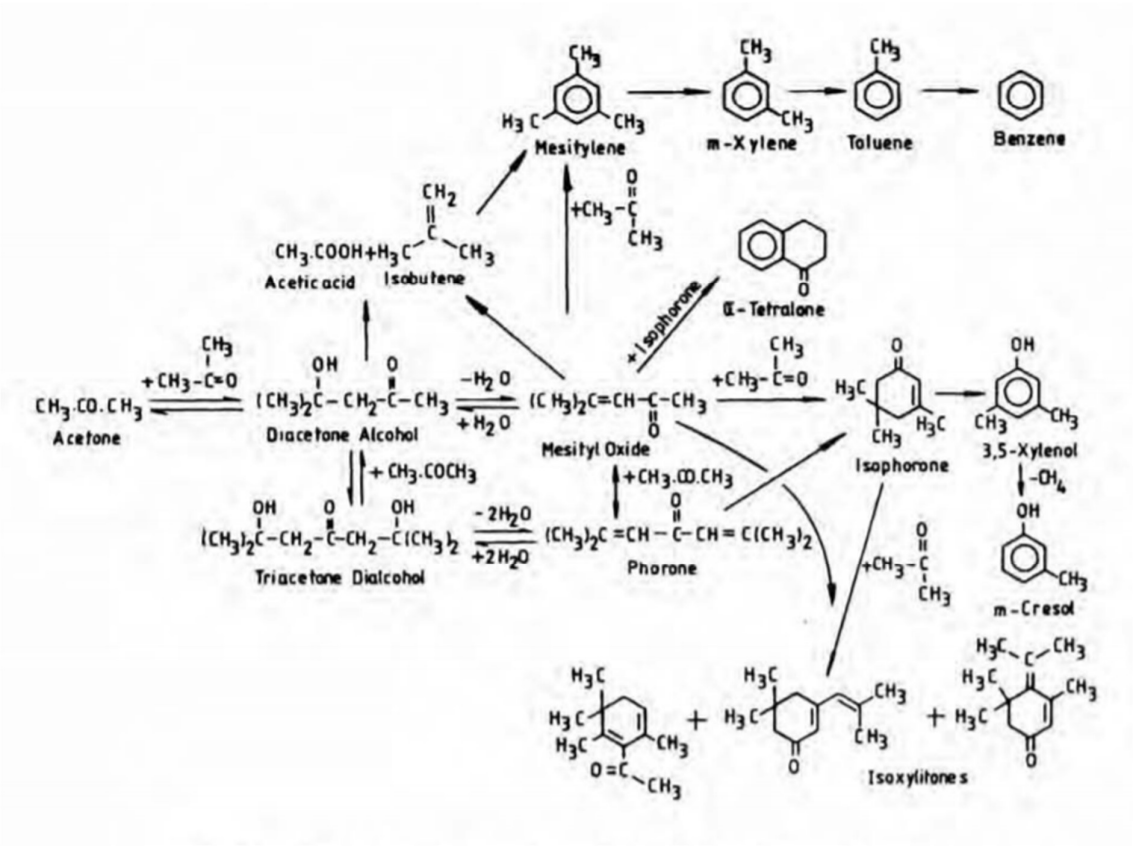


Figure 19 Image showing the Catalytic Cyclocondensation of Acetone to Isophorone (Ramanamurty and Salvapati, 1999)

Ethanol was the next solvent to be evaluated, with an inability to dissolve PVDF at room temperature, it was added to the vessel in the same volumes as the previous two solvents. With ethanol having

similar supercritical conditions of that of acetone it was a good comparison to see the difference in solvents compared to conditions. The anode was left in the same condition to that of the acetone runs, that being intact with the graphite easily removed. The ethanol stayed the same colour as when it was added, being clear and colourless. The main difference path and the colour was that there was a white suspension throughout the liquid. Multiple methods used to remove the white substance on suspension. The first was using a beaker of the liquid on a hot plate for approximately 10 minutes as the simplest removal, this caused the white substance to discolour so this method was not used again. The next was using a rotary evaporator to try and nullify the discolouration but this caused a different problem due to the white substance being extremely difficult to remove from the pear-shaped flask. The final method was using a vacuum pump conical flask and a ceramic filter to remove the powder without being damaged. This method was then used for future supercritical runs. The powder was then dried at 40°C in a drying oven. Once dried the powder resembled pure PVDF with slight black discolouration, this was put down to small flakes of graphite becoming dislodged from the anode material during processing.

The next step was to figure out the chemical structure of the white suspension which was postulated to be PVDF. Due to the chemical make-up of PVDF, there is the possibility that HF could be produced. HF is incredibly damaging to a lot of analytical techniques, this meant that there was only a small choice of analytical techniques that could be used. These were Light microscopy, thermogravimetric (TG-IR), infrared (IR) and scanning electron microscopy (SEM). These techniques gave a wide margin of analytical proof that what was being produced was PVDF. There were some problems at the beginning, which were found using TGIR and XRD. There were particles that would not break down at the temperature that PVDF breaks down and there were irregularities in the XRD spectrums that were being produced, these spectrums were not included in the report. This was caused by fibreglass which was stuck to the inside of the pressure vessel, left by other experiments being conducted within the vessel. A deeper clean was needed to remove the fibreglass from the vessel for new uncontaminated products to be produced. Correlated with that of Pure PVDF Figure 23, The infrared spectrum that is produced from the ethanol produced white substance has a very similar fingerprint region to that of PVDF. Using two different microscopy techniques light and scanning electron microscope, the particle size of the white substance being produced can be examined and compared to that of pure PVDF in Figure 20. Firstly, comparing images produced from the light microscope they have an almost identical structure. Very high surface area to volume ratio can be examined from both forming an almost fractal-like structure, this is seen in Figures 17 to 19. A deeper look at the structure using a scanning electron microscope shows that the white substance contains smaller particles than that of pure PVDF. Using the scanning electron microscope to examine the elements within the structure show that both

have a very similar elemental make-up of primarily carbon and fluorine. This is observed in Figures 27-30 and 35-38. Observing all the data that has been examined it can be proved that the supercritical extraction process does extract PVDF from the anode structure. The PVDF was extracted using the ethanol does have contaminant within its structure, there are traces of other element including, silicon, copper, sodium, aluminium, phosphorus, sulphur, chlorine and in large amounts of oxygen. Many of these can be explained by the fact that the PVDF was extracted from part of an electric car battery, where most of these elements are known to be present. The oxygen which is the highest-level pollutant is most likely caused by the extraction process, with the alcohol causing it to contaminate the PVDF with oxygen. From the level of oxygen, it is most likely found due to the depolymerisation process to create smaller particles of PVDF which in turn would then become dissolved within the supercritical ethanol extracting it from the anode's laminated structure. Now that it has been proven possible to extract PVDF from the anode more experimentation will be needed to see if other solvents are more efficient at extracting the PVDF from the anode.

Further tests were done using methanol, propanol, butanol, and DCM as other solvents using the same supercritical extraction methodology, described in section 4.2, the previously used solvents. Methanol is the first solvent to be tested and it produced a very similar anode material after processing to that of acetone and ethanol. Unlike those to there is no discolouration in Figure 18. Light microscopy images showed that the PVDF that was being produced seemed to contain smaller particles with less surface area than that of pure PVDF Figure 20 or ethanol produced PVDF Figure 21. This could be due to the decreased solvent ability compared to that of ethanol or acetone. The PVDF produced using methanol gave off a similar infrared spectra to that of ethanol produced PVDF shown in Figure 24 and Figure 26. The contaminants causing the carboxylic acids spike is not present in the methanol recovered PVDF Figure 24. There was an increase for elemental contaminant in the methanol extraction Figure 37. Showing almost 3 times the amount of oxygen and a larger amount of copper than ethanol Figure 41. The increased amount of oxygen could be due to the decreased particle size of the polymer, as seen in comparing the sizes in the SEM Figure 34 and Figure 38 showing that more depolymerisation has taken place compared to that of the ethanol extraction. The abundance of copper compared to extraction could be due to the increased use of the copper as a catalyst for the depolymerisation or that the use of ethanol caused more damage to the laminated copper layer.

When propanol was used a very small fraction, less than 0.1g of PVDF could be recovered. Another propanol run would be needed in the future to fully examine the use of propanol in the extraction of PVDF. Butanol extracted PVDF when examined seems to follow a pattern to the opposite of methanol extracted PVDF. The particles form seemed to be larger with some very small particles, this can be viewed through the images from the light microscope Figure 22 and the scanning electron microscope

Figure 46. The amount of oxygen contaminating the butanol produced PVDF Figure 48 is almost half that of ethanol produced PVDF Figure 41. It would be interesting the future to test larger alcohol molecules to determine the maximum reduction of oxygen reduced PVDF.

Finally, DCM was used to extract PVDF, as another strong solvent it would be interesting to compare this to alcohol and acetone solvents. The anode material after extraction takes place is more damaged than that of the other solvents. Under a light microscope the PVDF produced is plate- like Figure 22. The plates produced can be imagined to be very similar to that which is using the actual anode material. Like with the use of acetone, there is some contamination from graphite more than that of acetone. This can be seen under scanning electron microscope as dark crystals Figure 49 containing only carbon and no other elements Figure 51. The PVDF produced using DCM had zero oxygen contamination and less contamination from other elements Figure 51. Overall, more repeats need to be done on each of the solvent especially propanol to determine an overall pattern for PVDF extraction.

5.2 Light Microscopy

Images generated from the analysis of PVDF produced from different supercritical solvents, showing different particle structures formed when using different solvents during the supercritical separation process.

As discussed in (Yeo and Kiran, 2005) these are the solid particles of the solid plastic that have dropped out of solution due to the decrease in the pressure and temperature of the reaction vessel. Once the solvent used had dropped out of supercritical conditions the solid plastic will have precipitated and formed a solid-liquid solution. The images shown in the below figures show the formed solid plastic.

All PVDF particles were dried out thoroughly before analysis. The pure PVDF shown in Figure 20 is an example of what a reusable PVDF product should look like, without processing.

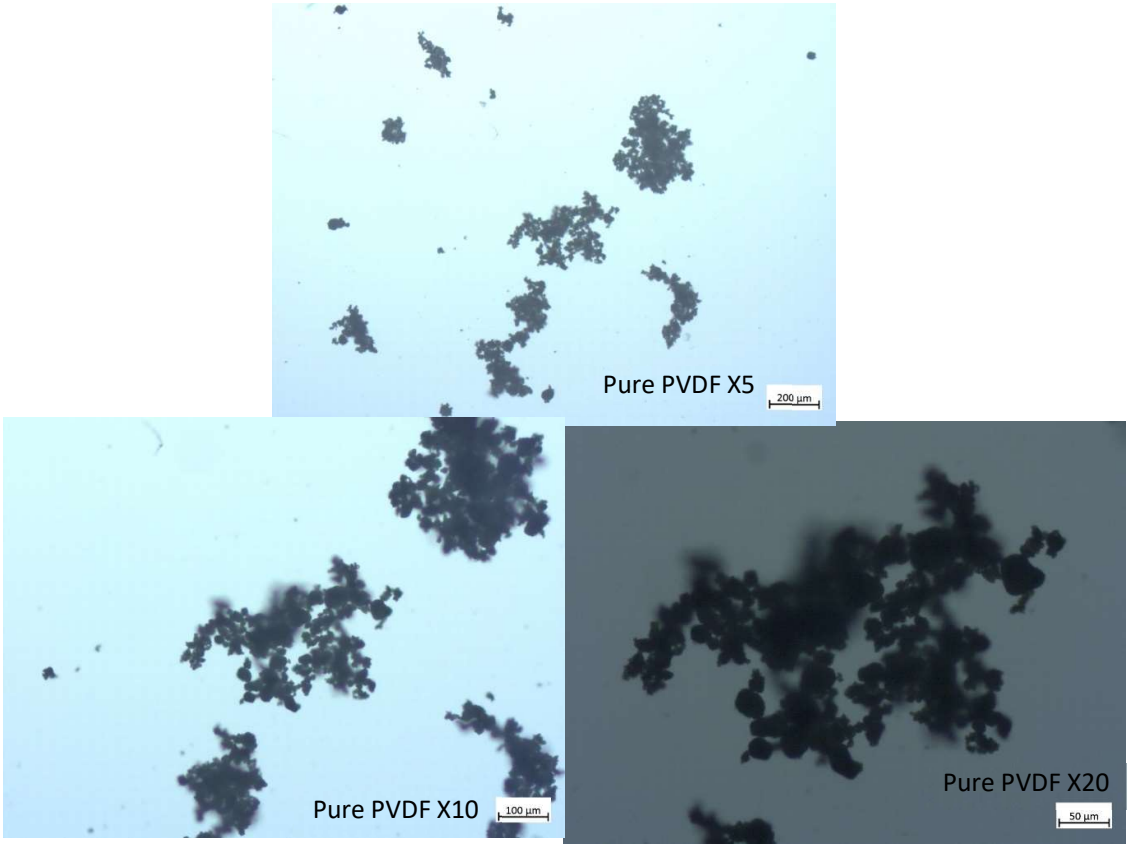


Figure 20 Images showing pure PVDF (no processing) at zooms from x5 to x20.

Figure 21 shows the products that have been produced using methanol and ethanol as the solvents during supercritical extraction from the anode. Methanol and ethanol producing a comparable size to that of the unprocessed PVDF. Giving the conclusion that the drying and extraction process could give a similar product to that of pure PVDF. More work would be needed to evaluate if the product produced could be reused in a similar manor to that of the original.

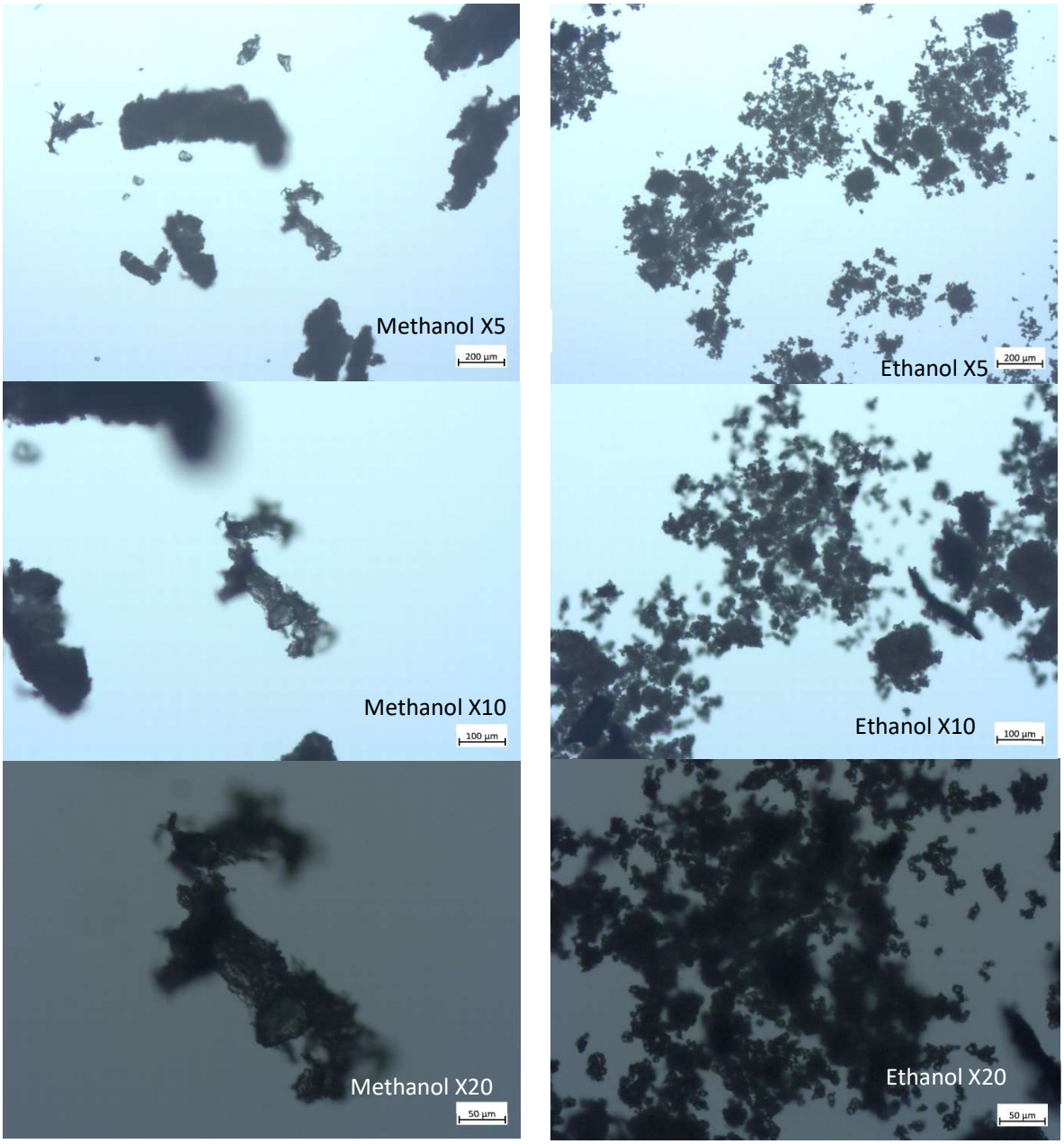


Figure 21 Images of PVDF recovered after processing in Methanol at 91 bar and 250 °C and Ethanol at 69 bar and 250 °C

Propanol as described previously was not able to give a usable product from SC extraction. The PVDF from the butanol solvent as seen in Figure 22, gave a smaller particle sizes to that of the product of methanol and ethanol SC extraction. Reasons for this being the case will need to be evaluated. The DCM SC extraction product gave a completely different visual structure as seen in Figure 22. The reasons behind this are unclear, the product was dried and processed in the same way to that of the previous examples.

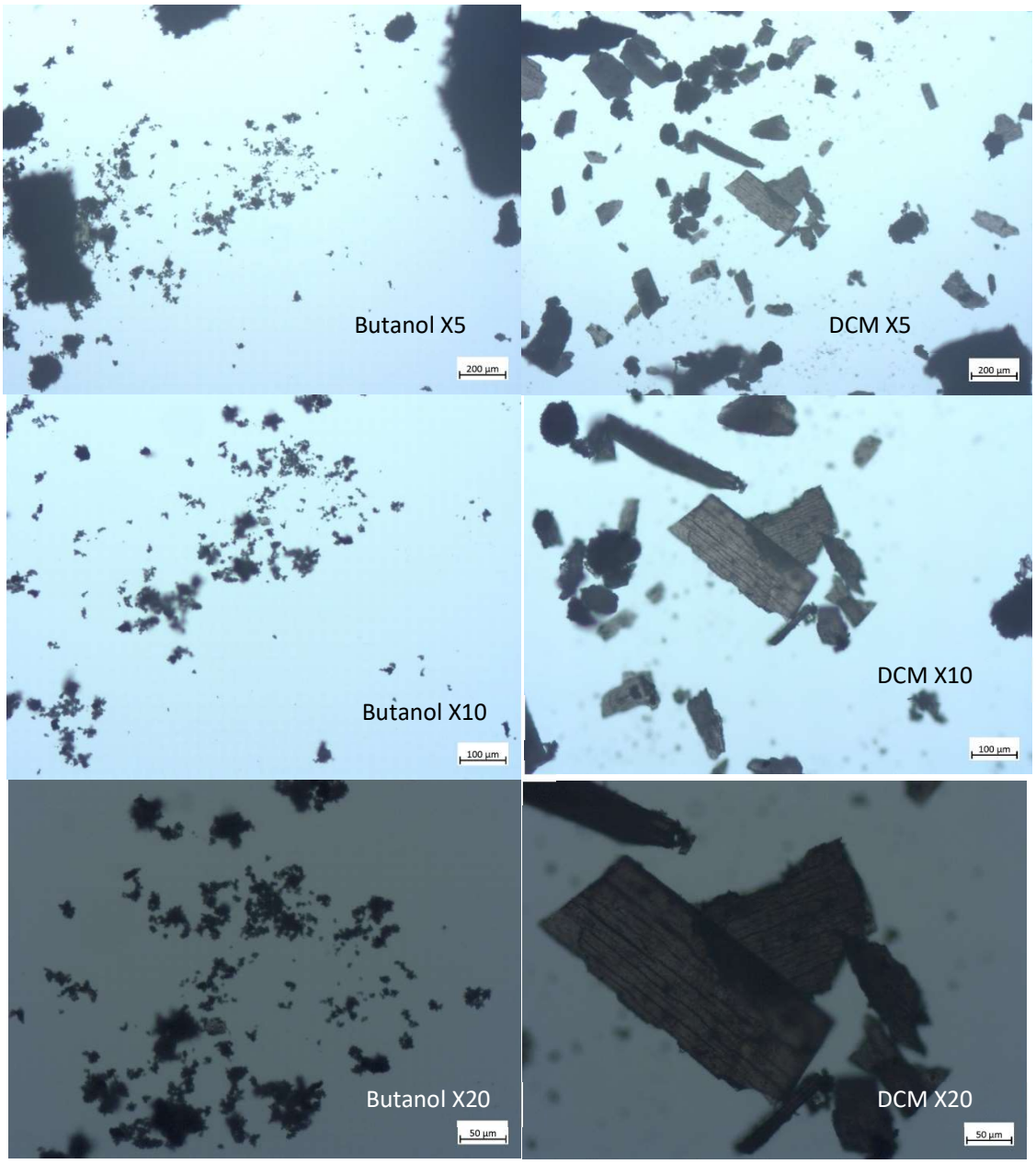


Figure 22 Images of PVDF recovered after processing in butanol at 56 bar at 290 °C and DCM at 67 bar at 250 °C

The images seen above layout the idea that the products being produced could be that of PVDF, but more evidence was required, Infra-red and SEM-EDS were used to determine the bonds and elemental analysis of the products being produced, to determine if the PVDF was extracted. Table 6 shows the average particle size of the precipitated plastic. The size of the plastic particles seems to decrease in size with the increase in the molecule size of the solvent. The reason for this will require future work along with the testing of the plastic to see if through this precipitating process it can be added back into production.

Table 6 Average particle sizes from light microscopy

Solvent	Particle Sizes (µm)			
	1	2	3	Average
Pure	400	350	450	400
Methanol	625	475	525	542
Ethanol	150	125	75	117
Butanol	62.5	37.5	50	50
DCM	550	525	475	517

5.3 Thermogravimetric and Infra-red

Thermogravimetric processing was conducted before infra-red analysis so to effectively separate the products required for infra-red analysis. Spectrums were generated using infra-red so that they could be compared to a library PVDF spectrum to see if the white solid that was extracted is PVDF and to see how the structure has changed through extraction. The other reason was to test the product for the possibility of glass fibre contamination. As the glass fibre wouldn't breakdown thermally unlike the PVDF. There was found to be some contamination due to a previous experiment, so further deep cleaning was required before moving forward with any further PVDF extraction experiments.

Infra-red spectroscopy was conducted on all the SC extraction products which can all be seen below. These spectrums are being compared to Figure 23 which has been taken from literature. Line A is what we are comparing it to as this is the pure PVDF spectrum. The spectrums are being used to locate the three main bonds within PVDF, these bonds can be seen in Figure 2. The labelling of these bonds CH_2, C-F and C-C have been placed on each of these spectrums. With C-F being the most important to find as this gives more proof that the SC extraction products are PVDF.

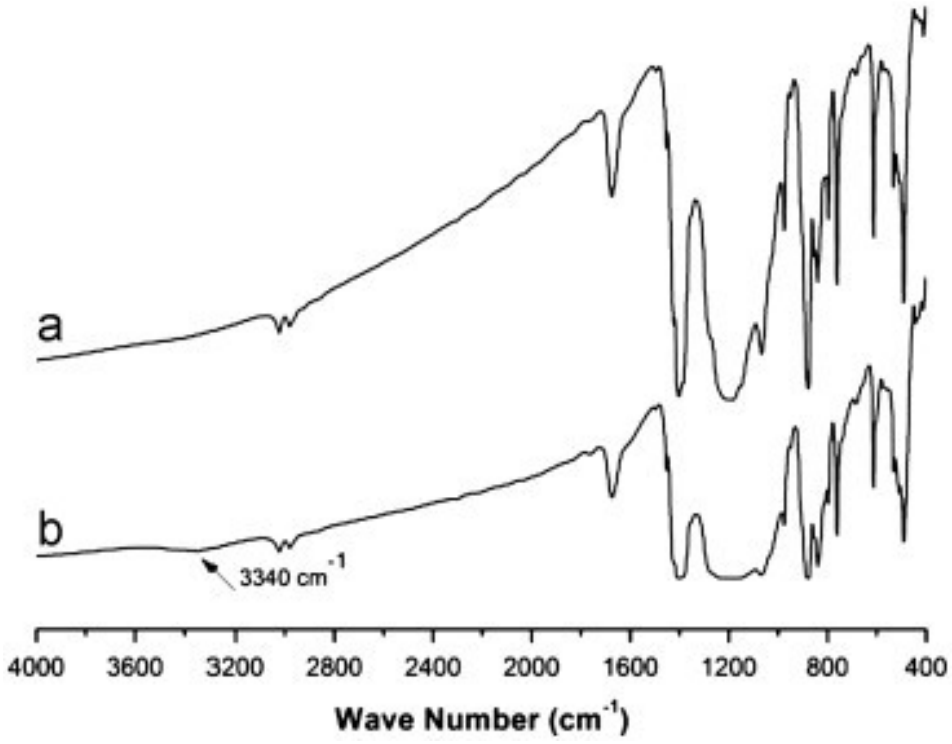


Figure 23 InfraRed spectrum of Pure PVDF (a) Composite membranes composite membranes blended with nano-crystalline cellulose (b) (Bai *et al.*, 2012)

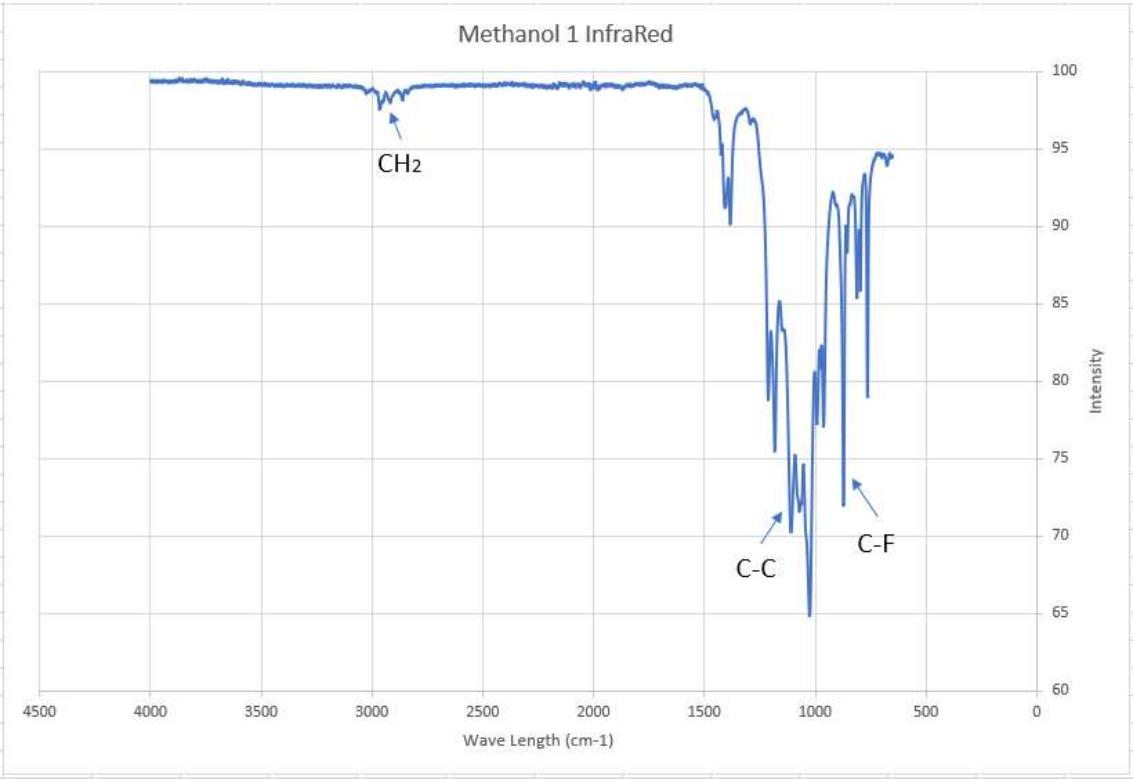


Figure 24 InfraRed Spectrum from Methanol extracted PVDF at 91 bar and 250 °C

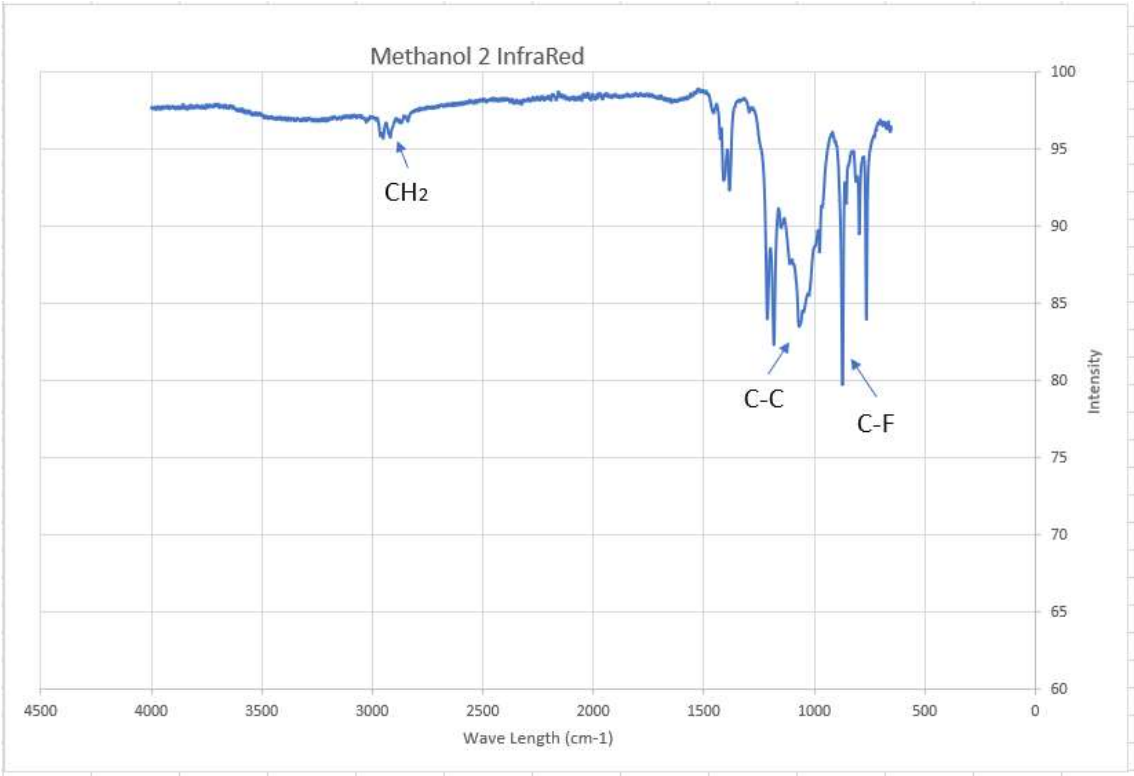


Figure 25 InfraRed Spectrum from Methanol extracted PVDF at 91 bar and 250 °C

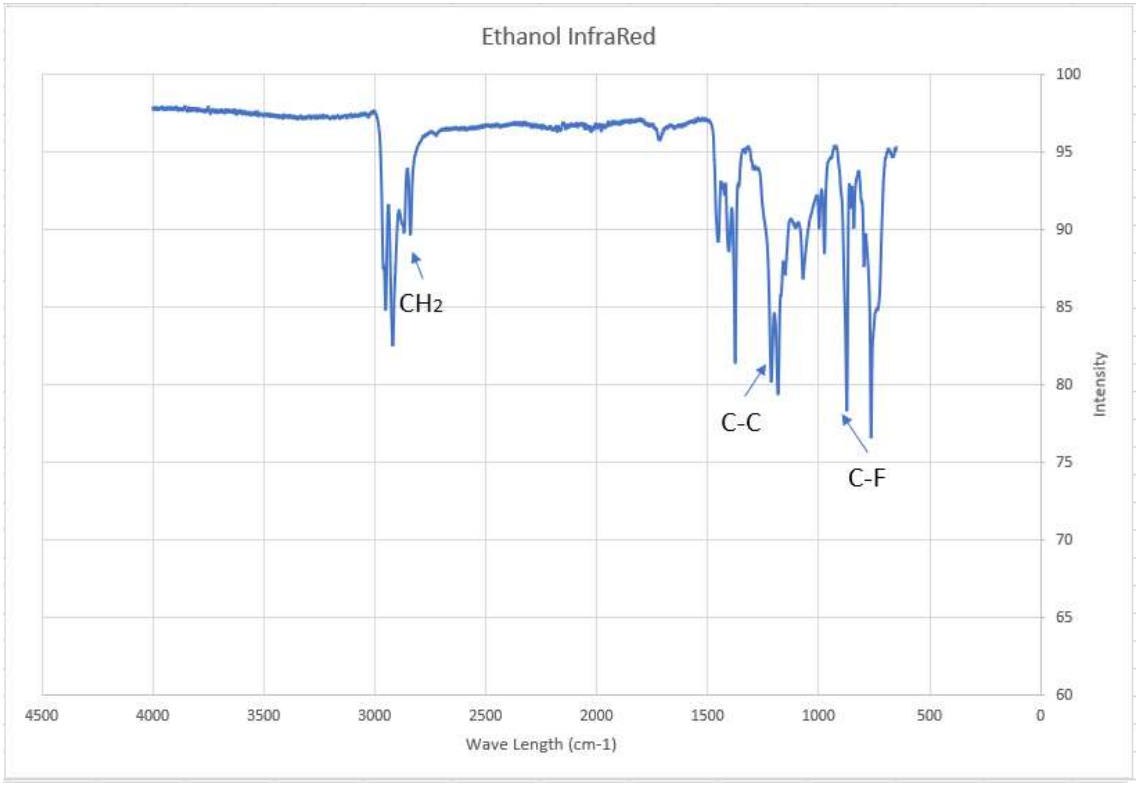


Figure 26 InfraRed Spectrum from Ethanol extracted PVDF at 69 bar and 250 °C

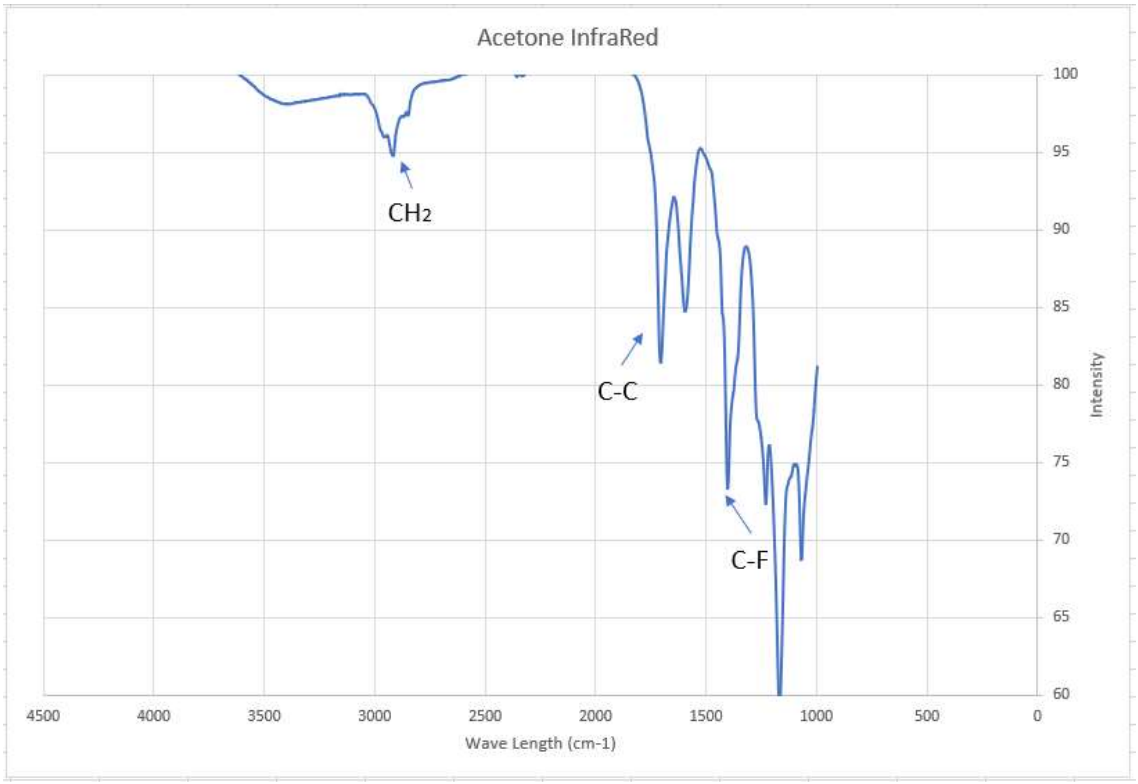


Figure 27 InfraRed Spectrum from Acetone extracted PVDF at 70 bar at 270 °C

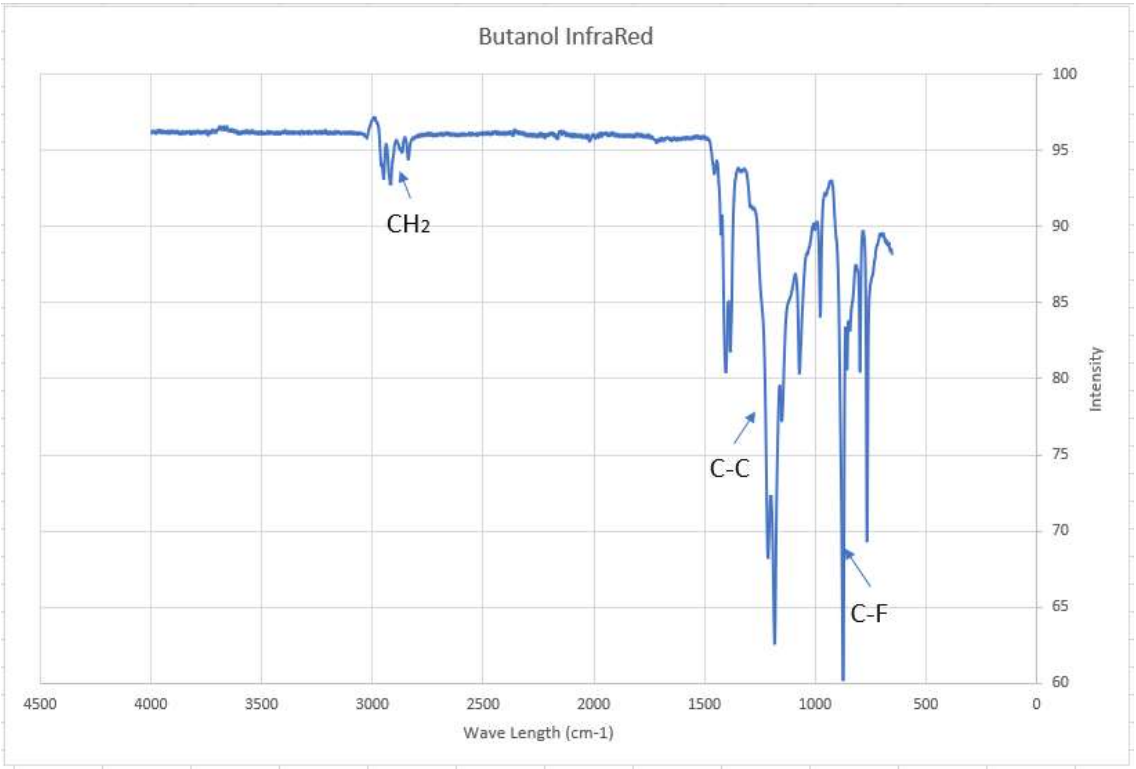


Figure 28 InfraRed Spectrum from Butanol extracted PVDF at 56 bar at 290 °C

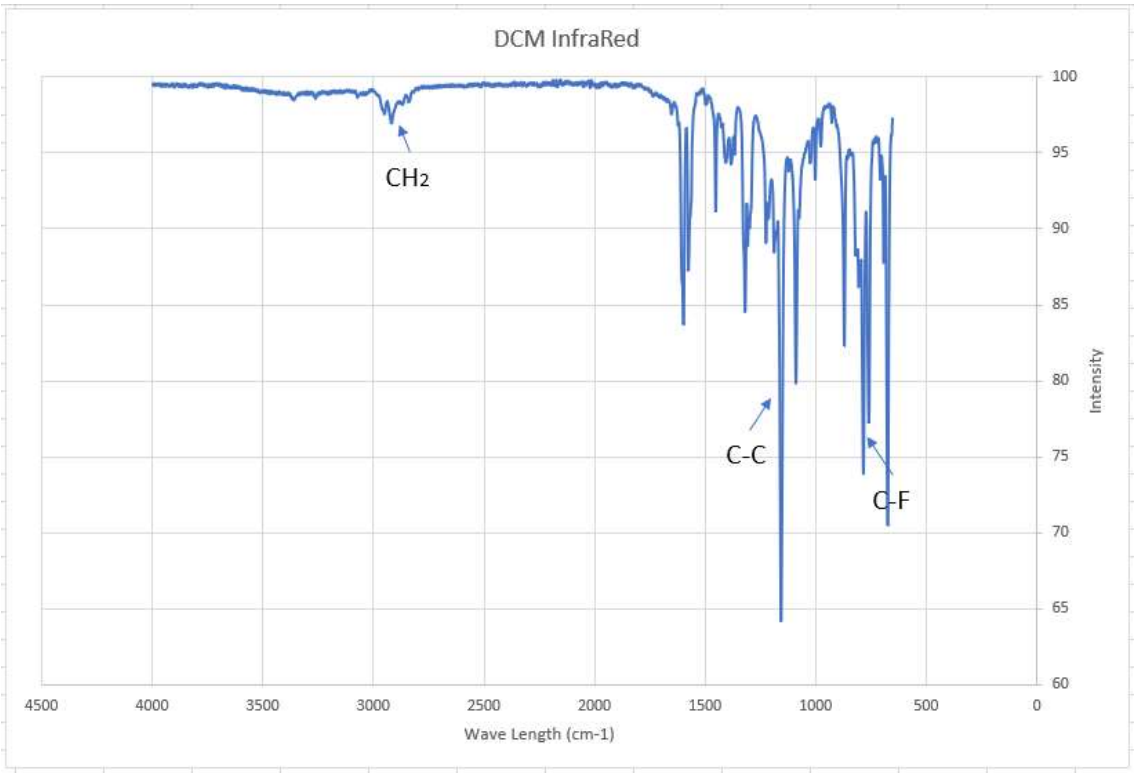


Figure 29 InfraRed Spectrum from DCM extracted PVDF at 67 bar at 250 °C

As a summary for the data that has been recorded from the Infrared analysis, Table 7 shows what peaks have been recorded and the maximum intensity of those peaks. From all solvent products the key three peaks were visible in each of them. This gives evidence to the conclusion that all these products are or at least contain PVDF. The data and spectrum of Acetone shown in Figure 27, will need to be redone to make sure that this wasn't an error in the collection of the results. If it is not, then it could be due to the PVDF being contaminated by the production of Isophorone as described in Figure 19. The value of the intensity of the peaks seem to follow no similar pattern that can be seen below in Table 7.

Table 7 Overall Data for solvent SC extraction products for Infrared Analysis

Solvent	Peaks Visible			Max Peak Intensity (cm-1)		
	CH2	C-C	C-F	CH2	C-C	C-F
Methanol	Yes	Yes	Yes	97.4	64.8	72.1
Ethanol	Yes	Yes	Yes	82.4	79.3	76.9
Acetone	Yes	Yes	Yes	94.8	81.7	73.8
Butanol	Yes	Yes	Yes	93.5	63.0	60.2
DCM	Yes	Yes	Yes	96.9	64.1	74.2

5.4 Scanning Electron Microscopy (SEM)

Using scanning electron microscopy and energy dispersive X-ray, it will be possible to view the particle structure and elemental analysis to be able to confirm if the solid product that was produced through supercritical extraction was PVDF. The elemental analysis will show distribution on a 3D image of the particles produced and a weight distribution of those elements.

5.4.1 SEM-EDX Data from Pure PVDF

The data being shown uses Pure PVDF, so that the supercritical extraction produced PVDF can be compared on purity and particle structure. The first image of each set of SEM-EDX data shows a 3D image of the PVDF or SC extraction product. For Pure PVDF this is shown as Figure 30. The next image shows a layered image containing the elements represented as Figure 31. The separate elements are show in Figure 32 with images showing the location of separate elements as separate images and colours. Figure 31 is the layered image version of Figure 32. Figure 33 describes the elemental analysis given as a EDX spectrum and table with weight and atomic percentages. These have been done for every product of supercritical extraction. With an overview of the elemental analysis at the end.

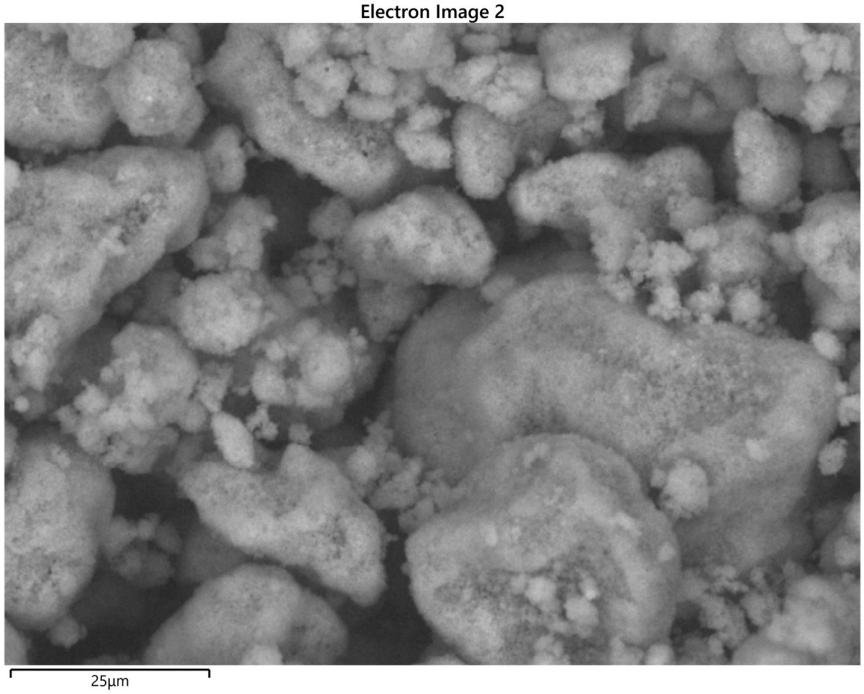


Figure 30 Image from Scanning Electron Microscope of Pure PVDF

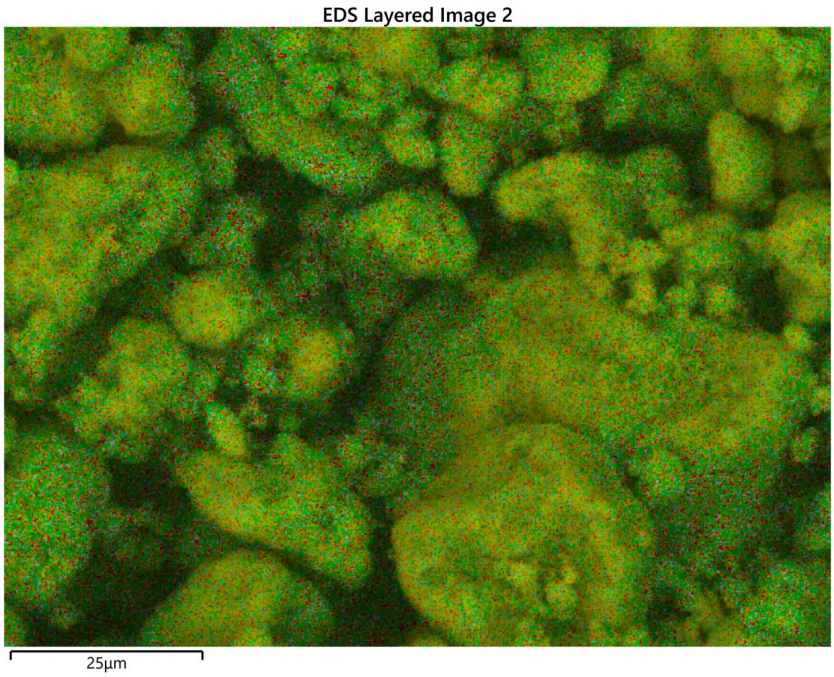


Figure 31 Image from Scanning Electron Microscope of Pure PVDF with Elemental Analysis overpage

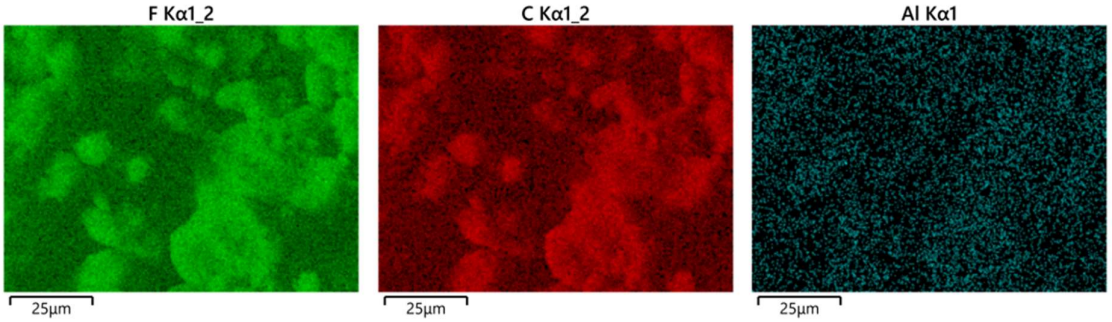
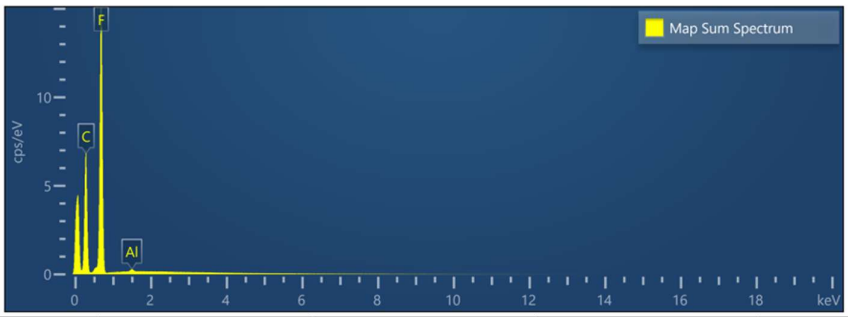


Figure 32 Images from Scanning Electron Microscope of Pure PVDF with individual element colour representations; Fluorine, Carbon, and Aluminium



Map Sum Spectrum				
Element	**Line Type**	**Weight %**	**Weight % Sigma**	**Atomic %**
C	K series	44.92	0.11	56.36
F	K series	54.85	0.11	43.51
Al	K series	0.23	0.01	0.13
Total		100.00		100.00

Figure 33 Elemental Analysis of Pure PVDF

5.4.2 SEM-EDX Data from Methanol Extracted PVDF

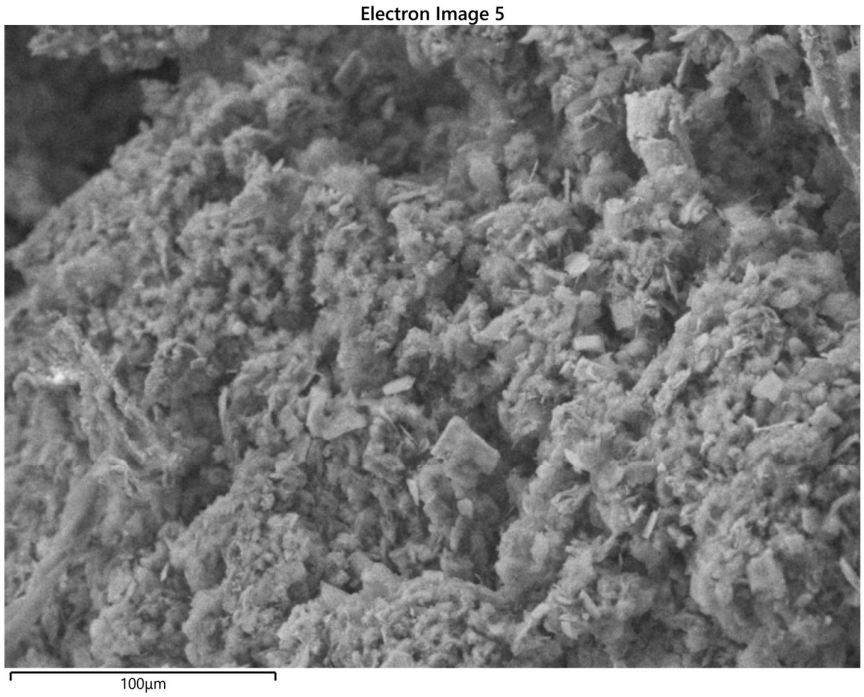


Figure 34 Image from Scanning Electron Microscope of Methanol Extracted PVDF at 91 bar and 250 °C

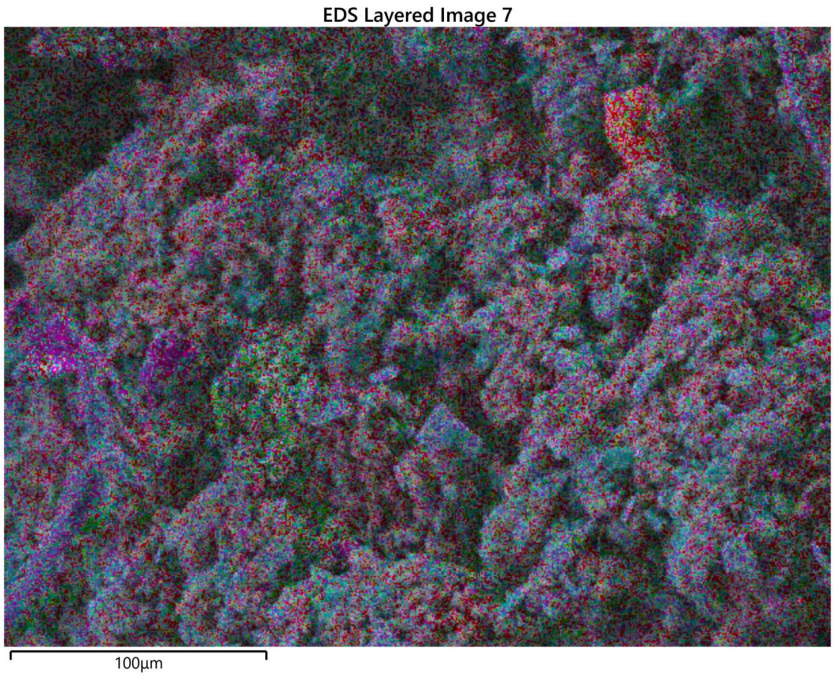


Figure 35 Image from Scanning Electron Microscope of Methanol Extracted PVDF at 91 bar and 250 °C with Elemental Analysis overpage

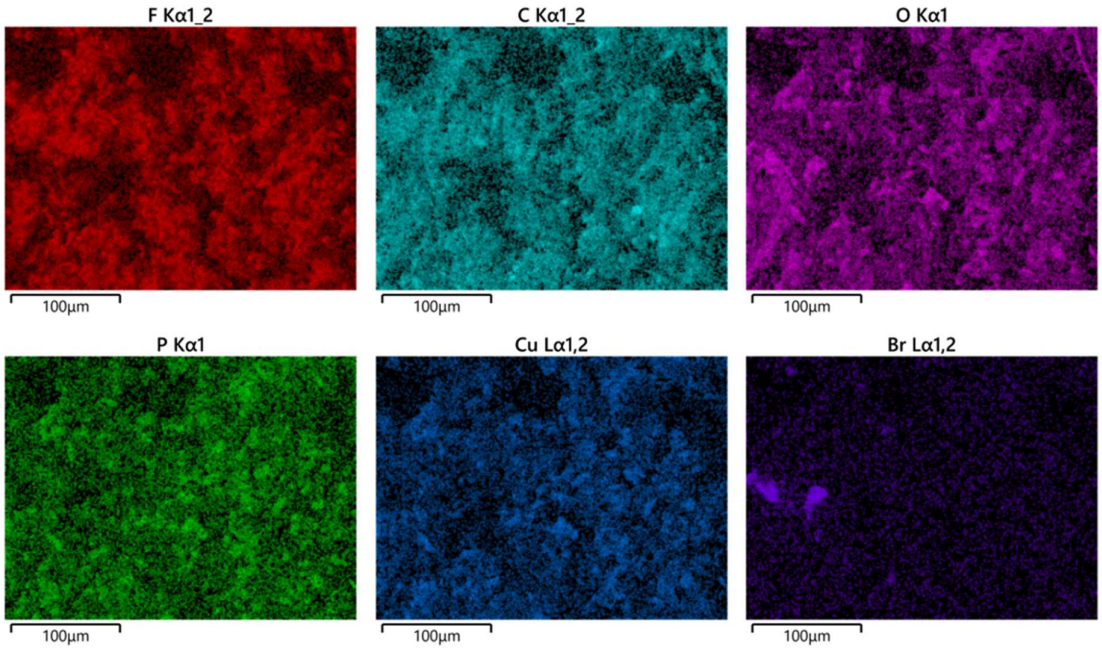
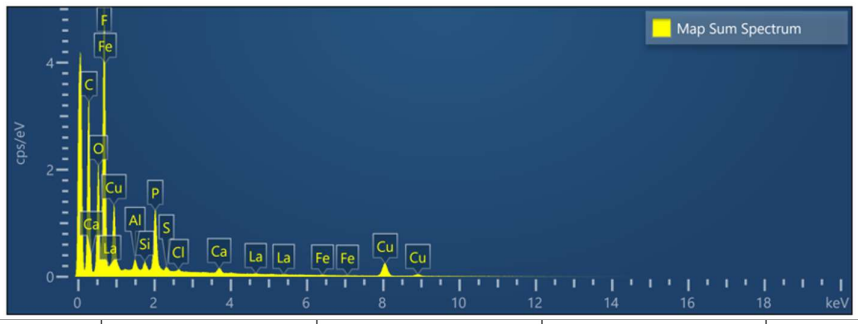


Figure 36 Images from Scanning Electron Microscope of Methanol Extracted PVDF at 91 bar and 250 °C with indivual element colour representations; Fluorine, Carbon, Oxygen, Phosphorus, Copper and Bromine.



Map Sum Spectrum				
Element	**Line Type**	**Weight %**	**Weight % Sigma**	**Atomic %**
C	K series	37.90	0.24	51.82
O	K series	14.71	0.15	15.10
F	K series	32.54	0.21	28.13
P	K series	2.72	0.03	1.44
Cu	L series	10.27	0.16	2.65
Si	K series	0.33	0.01	0.20
Ca	K series	0.39	0.02	0.16
S	K series	0.19	0.01	0.10
Cl	K series	0.11	0.01	0.05
Al	K series	0.46	0.02	0.28
La	L series	0.23	0.05	0.03
Fe	K series	0.13	0.03	0.04
Total		100.00		100.00

Figure 37 Data showing the Elemental Analysis of Methanol Extracted PVDF at 91 bar and 250 °C

5.4.3 SEM-EDX Data from Ethanol Extracted PVDF

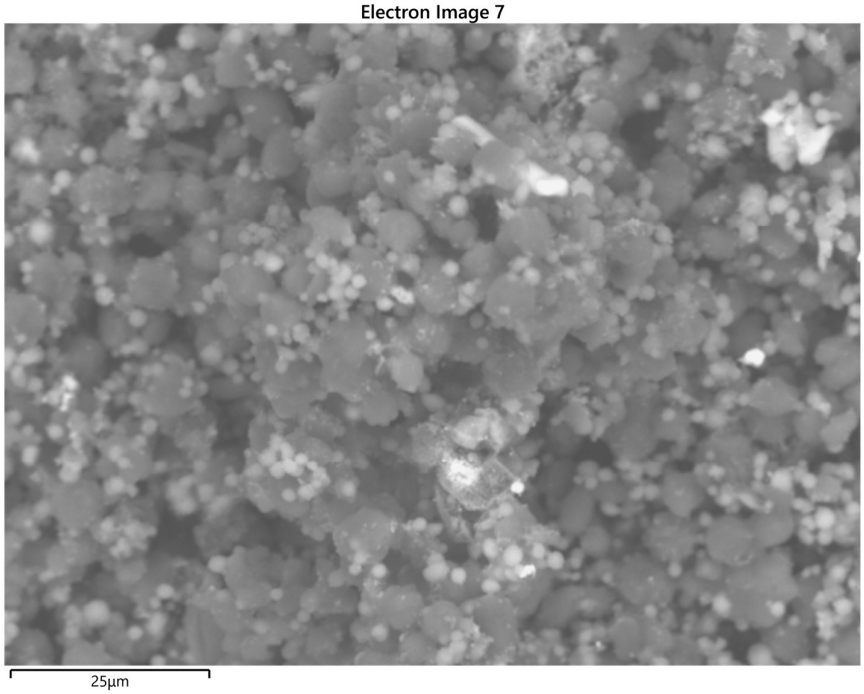


Figure 38 Image from Scanning Electron Microscope of Ethanol Extracted PVDF at 69 bar and 250 °C

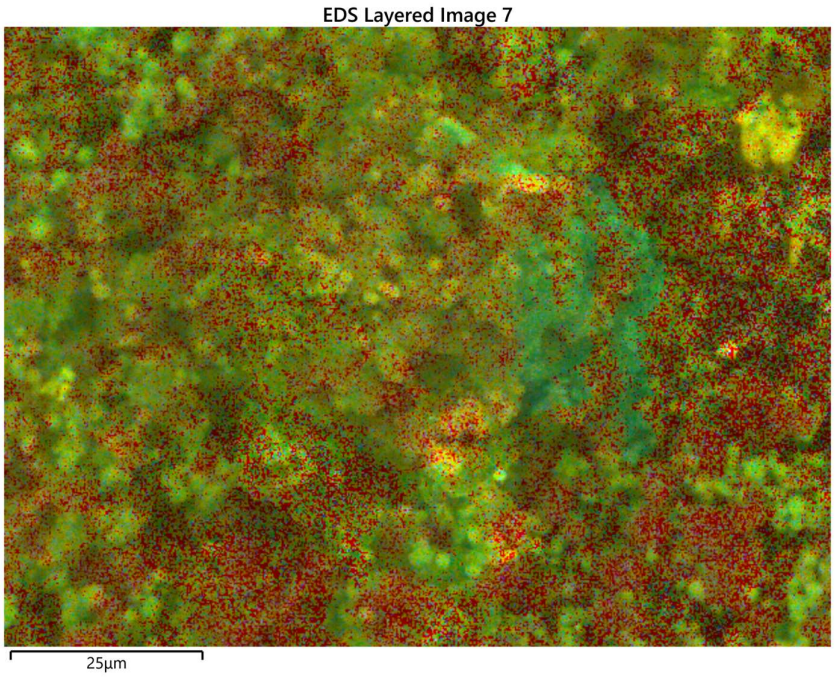


Figure 39 Image from Scanning Electron Microscope of Ethanol Extracted PVDF at 69 bar and 250 °C with Elemental Analysis overpage

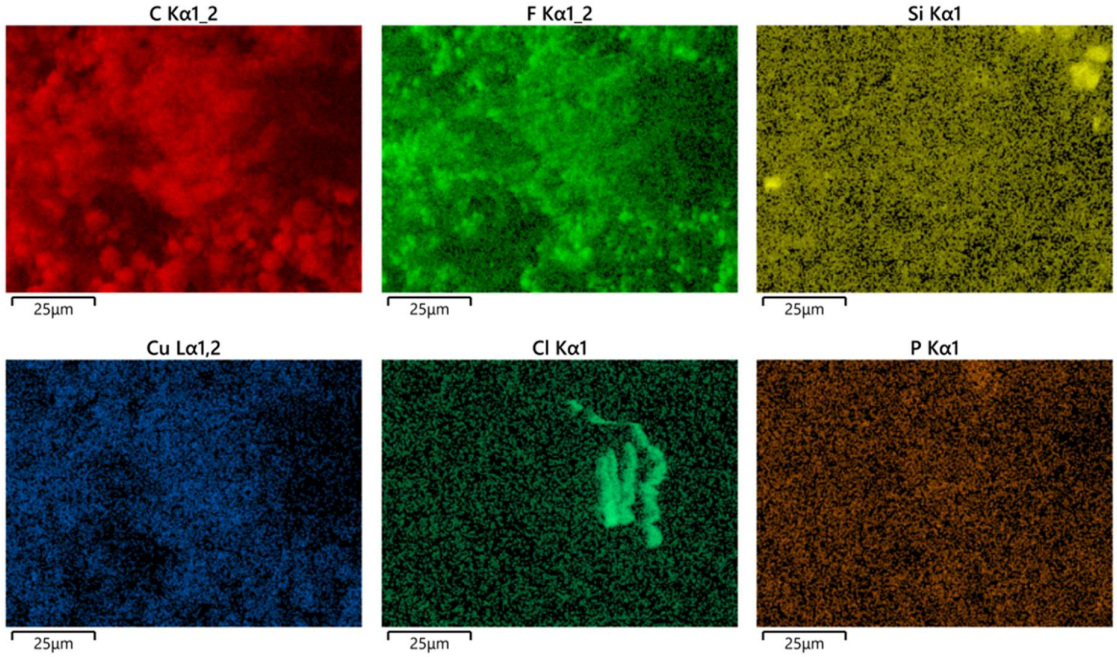
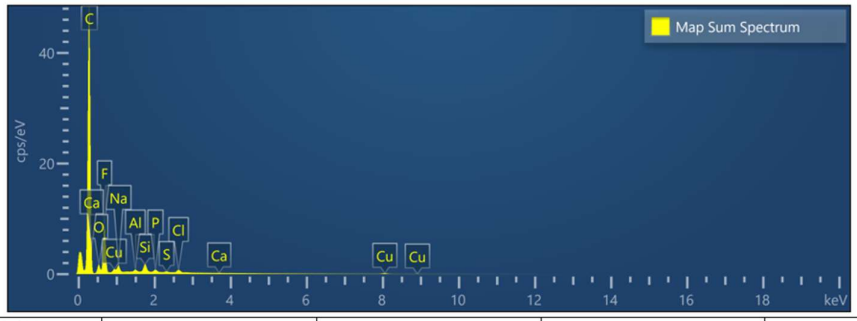


Figure 40 Images from Scanning Electron Microscope of Ethanol Extracted PVDF at 69 bar and 250 °C with indivual element colour representations: Carbon, Fluorine, Silicon, Copper, Chlorine, Phosphorus.



Map Sum Spectrum				
Element	**Line Type**	**Weight %**	**Weight % Sigma**	**Atomic %**
C	K series	75.05	0.09	83.01
F	K series	16.67	0.06	11.66
Si	K series	0.68	0.01	0.32
Cu	L series	1.16	0.04	0.24
Na	K series	0.87	0.01	0.51
Al	K series	0.18	0.01	0.09
P	K series	0.24	0.01	0.10
S	K series	0.08	0.01	0.03
Cl	K series	0.32	0.01	0.12
O	K series	4.71	0.07	3.91
Ca	K series	0.02	0.01	0.01
Total		100.00		100.00

Figure 41 Data showing the Elemental Analysis of Ethanol Extracted PVDF at 69 bar and 250 °C

5.4.4 SEM-EDX Data from Acetone Extracted PVDF

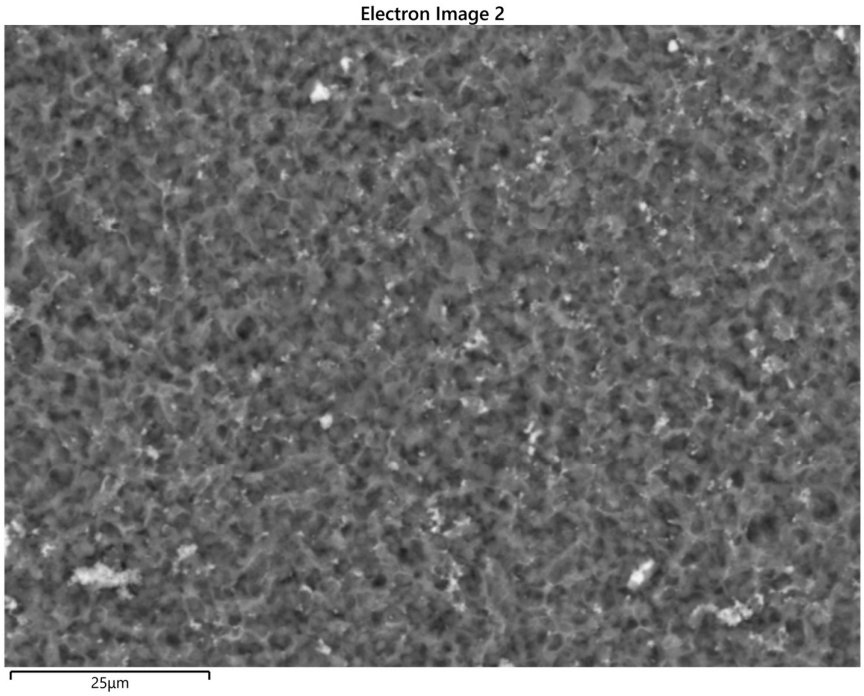


Figure 42 Image from Scanning Electron Microscope of Acetone Extracted PVDF

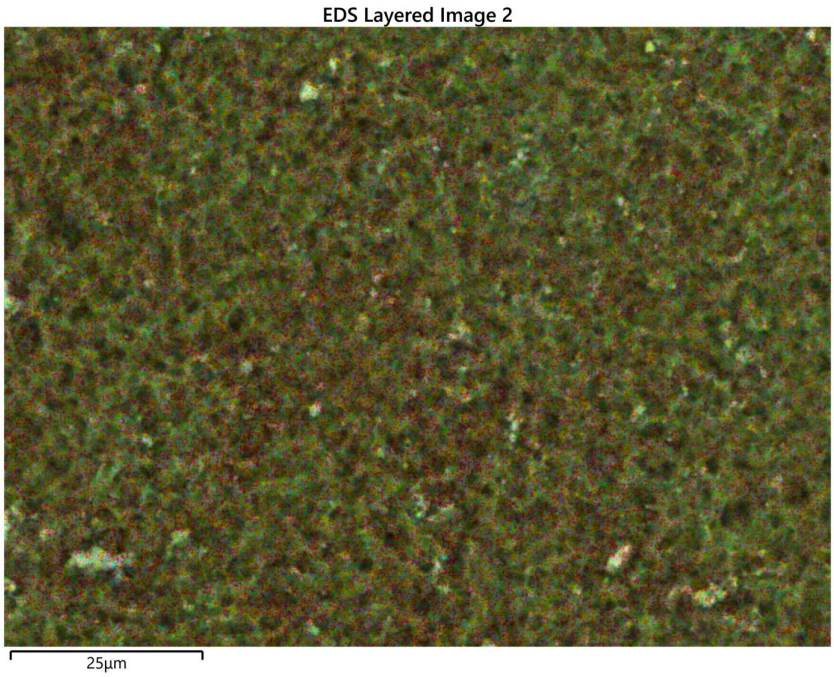


Figure 43 Image from Scanning Electron Microscope of Acetone Extracted PVDF with Elemental Analysis overpage

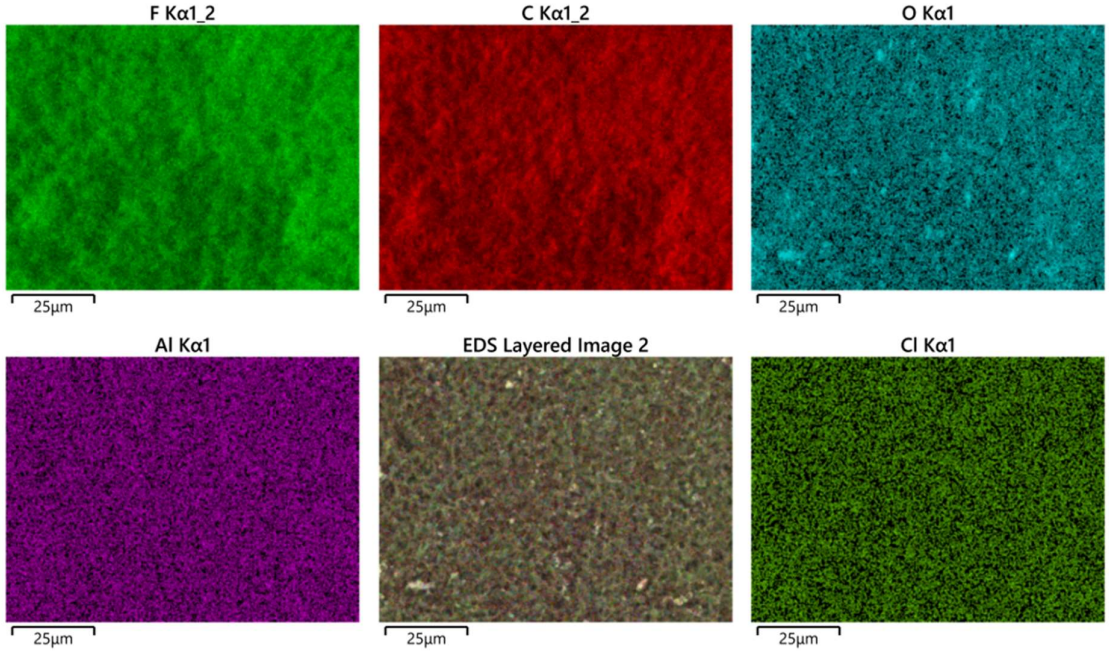
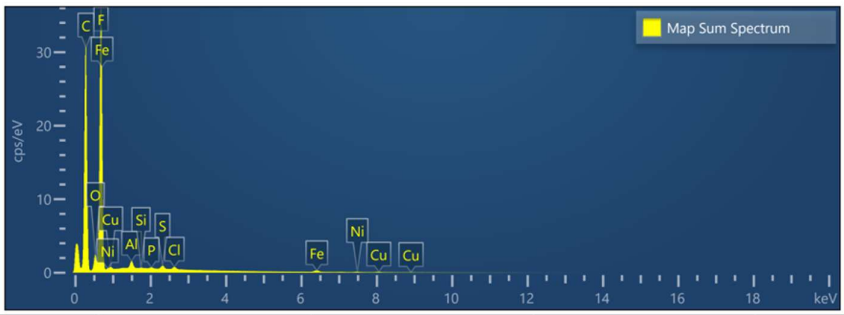


Figure 44 Images from Scanning Electron Microscope of Acetone Extracted PVDF with indivual element colour representations, Fluorine, Carbon, Oxygen, Aluminium and Chlorine



Map Sum Spectrum				
Element	Line Type	Weight %	Weight % Sigma	Atomic %
C	K series	51.01	0.08	62.49
O	K series	4.44	0.04	4.08
F	K series	42.06	0.08	32.57
Al	K series	0.45	0.01	0.25
S	K series	0.22	0.01	0.10
Fe	K series	0.67	0.02	0.18
Cu	L series	0.63	0.04	0.15
Cl	K series	0.19	0.01	0.08
P	K series	0.07	0.01	0.03
Ni	K series	0.23	0.02	0.06
Si	K series	0.02	0.01	0.01
Total		100.00		100.00

Figure 45 Data showing the Elemental Analysis of Acetone Extracted PVDF

5.4.5 SEM-EDX Data from Butanol Extracted PVDF

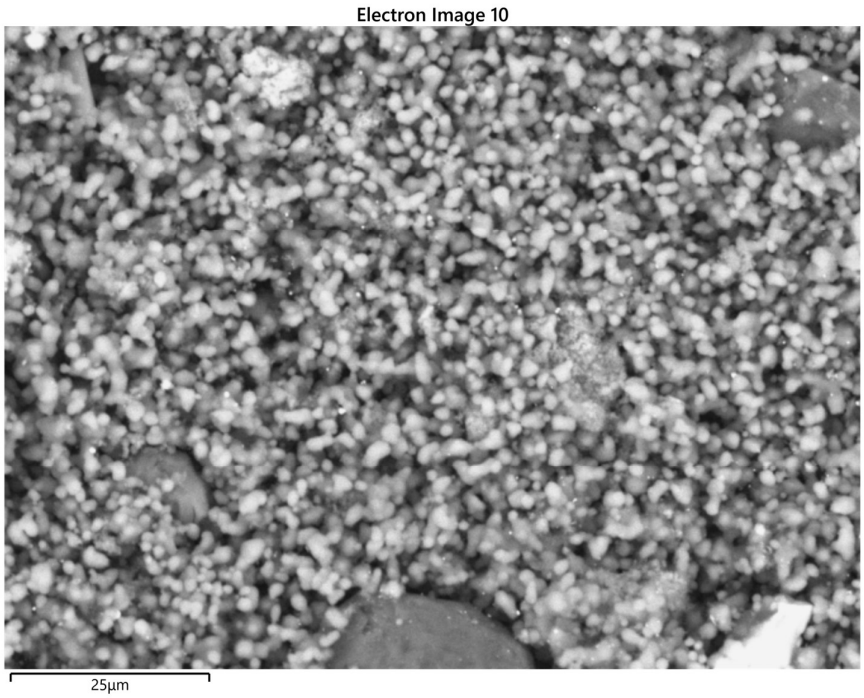


Figure 46 Image from Scanning Electron Microscope of Butanol Extracted PVDF at 56 bar at 290 °C

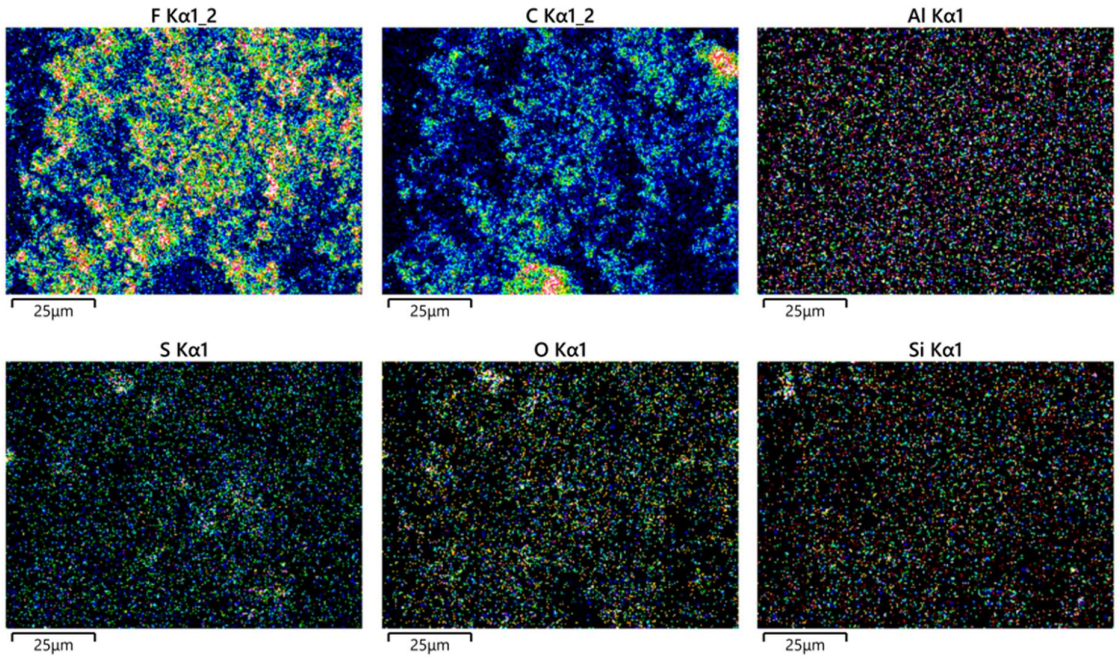
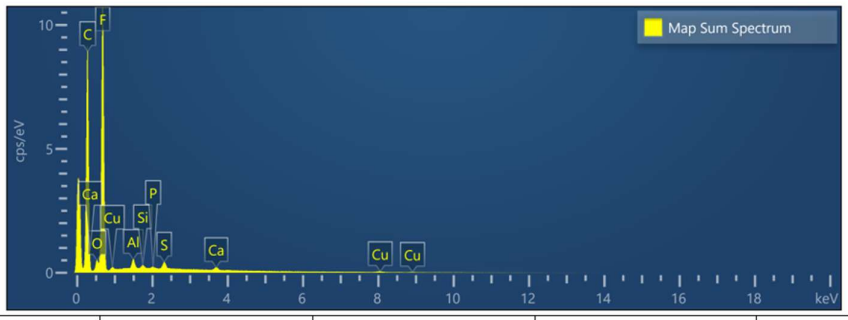


Figure 47 Images from Scanning Electron Microscope of Butanol Extracted PVDF at 56 bar at 290 °C with indivual element colour representations: Fluorine, Carbon, Aluminium, Silicon, Oxygen and Silicon



Map Sum Spectrum				
Element	Line Type	Weight %	Weight % Sigma	Atomic %
C	K series	52.47	0.18	63.94
F	K series	42.36	0.17	32.63
Al	K series	0.60	0.02	0.33
S	K series	0.47	0.02	0.22
O	K series	2.67	0.11	2.44
Cu	L series	0.80	0.07	0.18
Si	K series	0.18	0.02	0.09
Ca	K series	0.35	0.02	0.13
P	K series	0.09	0.02	0.04
Total		100.00		100.00

Figure 48 Data showing the Elemental Analysis of Butanol Extracted PVDF at 56 bar at 290 °C

5.4.6 SEM-EDS Data from DCM Extracted PVDF

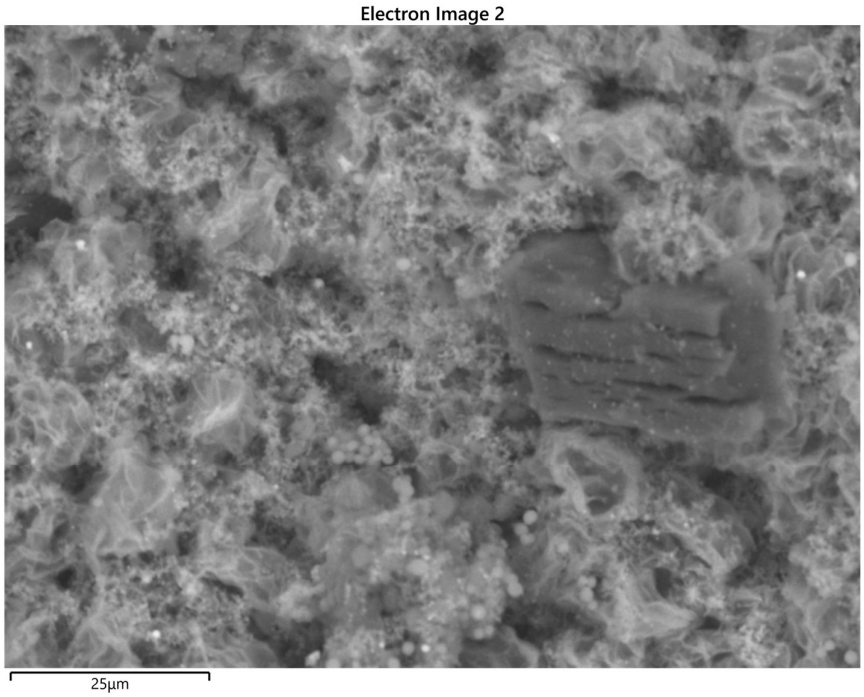


Figure 49 Image from Scanning Electron Microscope of DCM Extracted PVDF at 67 bar at 250 °C

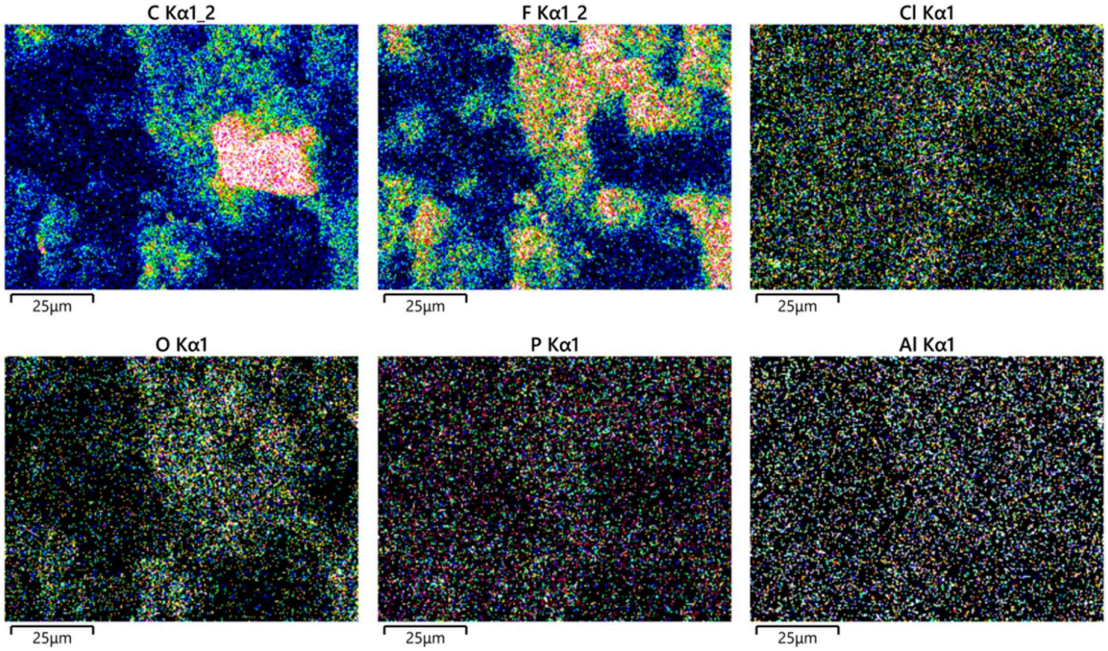
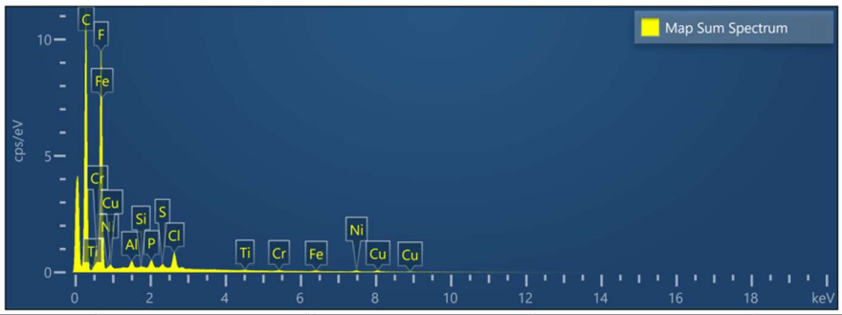


Figure 50 Images from Scanning Electron Microscope of DCM Extracted PVDF at 67 bar at 250 °C with indivual element colour representations: Carbon, Fluorine, Chlorine, Oxygen, Phosphorus and Aluminium.



Map Sum Spectrum				
Element	Line Type	Weight %	Weight % Sigma	Atomic %
C	K series	58.31	0.21	70.26
F	K series	36.82	0.20	28.05
Cl	K series	1.21	0.02	0.49
P	K series	0.50	0.02	0.23
S	K series	0.23	0.02	0.10
Cu	L series	1.09	0.09	0.25
Al	K series	0.41	0.02	0.22
Ni	K series	0.75	0.06	0.19
Cr	K series	0.21	0.03	0.06
Fe	K series	0.32	0.04	0.08
Si	K series	0.07	0.01	0.03
Ti	K series	0.09	0.02	0.03
Total		100.00		100.00

Figure 51 Data showing the Elemental Analysis of DCM Extracted PVDF at 67 bar at 250 °C

5.4.7 Overall SEM-EDS Data from Extracted PVDF

A collection of the atomic percentages from the EDX data has been shown below as Table 8. This has been taken from each individual data source. This is to compare and investigate the two types and sources of contamination for the SC extraction products.

The oxygen is a common contamination when looking at the solvents having oxygen. The source of the contamination will be due to the solvent, this is clear when seeing that there is no oxygen contamination when seeing the SC DCM product. The pattern seems to be that as the carbon value increases in the solvent, the oxygen contamination decreases. With the oxygen contamination being so high when using methanol compared to the other solvents, due to there being a higher atomic percentage of oxygen in the solvent itself. It is also possible that there is still some of the solvent left on the product after drying, but this is less likely than that the solvent has reacted with the product.

The rest of the contamination is a collection of other elements with no discernible pattern other than that the contamination seems to decrease in a similar manor to that of the oxygen. With smaller molecule alcohols having larger percentages of other element contaminants. These contaminants are more than likely due to the manufacturing of the anode material itself. More tests can be done to

determine the exact source, but with this being the only discernible difference between the SC products and the pure product, it can be concluded these were introduced due to the anodes structure.

Table 8 Overall SEM-EDS Data from Extracted PVDF showing Elemental Atomic %

Element	Atomic % from PVDF Supercritical Extraction of					
	Pure PVDF	Methanol	Ethanol	Acetone	Butanol	DCM
Carbon	56.36	51.82	83.01	62.49	63.94	70.26
Fluorine	43.51	28.13	11.66	32.57	32.63	28.05
Oxygen	0.00	15.10	3.91	4.08	2.44	0.00
Other	0.13	4.95	1.42	0.86	0.99	1.69
Total	100.00	100.00	100.00	100.00	100.00	100.00

5.5 Tunnelling Electron Microscopy (TEM)

To upgrade the clean graphite once PVDF has been removed, strategies to produce graphene were investigated on both new battery grade graphite and end-of-life graphite from anode material. The use of ethanol at supercritical conditions was used to separate the graphite layers to produce graphene. Two methods were investigated using the supercritical solvents: the use of an ultrasonic probe and the use of a rapid pressure release valve. The use of a 1 L high-pressure vessel was used for the supercritical separation container, the same temperature control system was used for this reactor as was used for the previous experiments with PVDF. The main difference with this vessel was that it had an inbuilt ultrasonic probe. There are two exit valves: one safety valve and another valve. The flow diagram shown in figure 7 was constructed and used for both processes. The ultrasonic probe was used before supercritical conditions and after so that an overview of the possibility of producing graphene using this process could be determined. Due to problems with the Sonic probe's control system only one feasibility run using the ultrasonic probe could be conducted. More experimentation with this method would be needed to investigate its use in the production of graphene using end-of-life graphite. The results from the first run were inconclusive due to reasons that will be described later.

The use of a rapid pressure release while the solvent was at supercritical conditions was to rip the layers of the graphite apart to produce graphene. The ultrasonic probe was not used, the ethanol was allowed to reach supercritical conditions kept it therefore five-minute and then the valves were opened allowing flow into the gas container. Once the noise of releasing gas had stopped the valves were closed and the gas container was plunged into cold water until reaching room temperature. The liquid contained within the gas container was then emptied into a sealed glass container and transported to a centrifuge so that the graphene nanoparticles could be easily discovered. The gas container was then transported to another department so that it could be an examined under a tunnelling electron microscope. The first attempt at this didn't create any results due to the graphene becoming too diluted within the liquid. This is the reason that the first run from the ultrasonic process came back with no results. Further attempts were done using both end-of-life and new graphite but this time there was a smaller window of time for the graphene to settle and further steps were taken to increase the concentration of graphene by increasing the graphite added to the vessel. There was approximately 1g per 150ml.

This time when using the tunnelling electron microscope images of graphene layers could be imaged and these can be seen in Figures 50-52. The images showing the new graphite show layers that seem to be thicker. They were also more difficult to be found. This is most likely due to the stronger intermolecular forces between the layers compared to that of end-of-life graphite. Literature (Chen

et al., 2017) says that end-of-life graphite due to the constant use and charging of the batteries the graphite layers have become weakened. This does seem to be the case when looking at the images from end-of-life graphite which were both easier to find and showed thinner layers.

Overall, the attempt to process graphite into graphene seems to be possible from the use of end-of-life graphite. More investigation needs to go into finding a way to capture and produce more of the graphene product without it settling back into graphite. Due to graphene being unstable in high concentrations, moving towards becoming graphite again. The use of analytical techniques such as Raman should be used in the future to possibly produce a pattern of how changing the conditions of the experiment could affect the layering of the graphene product.

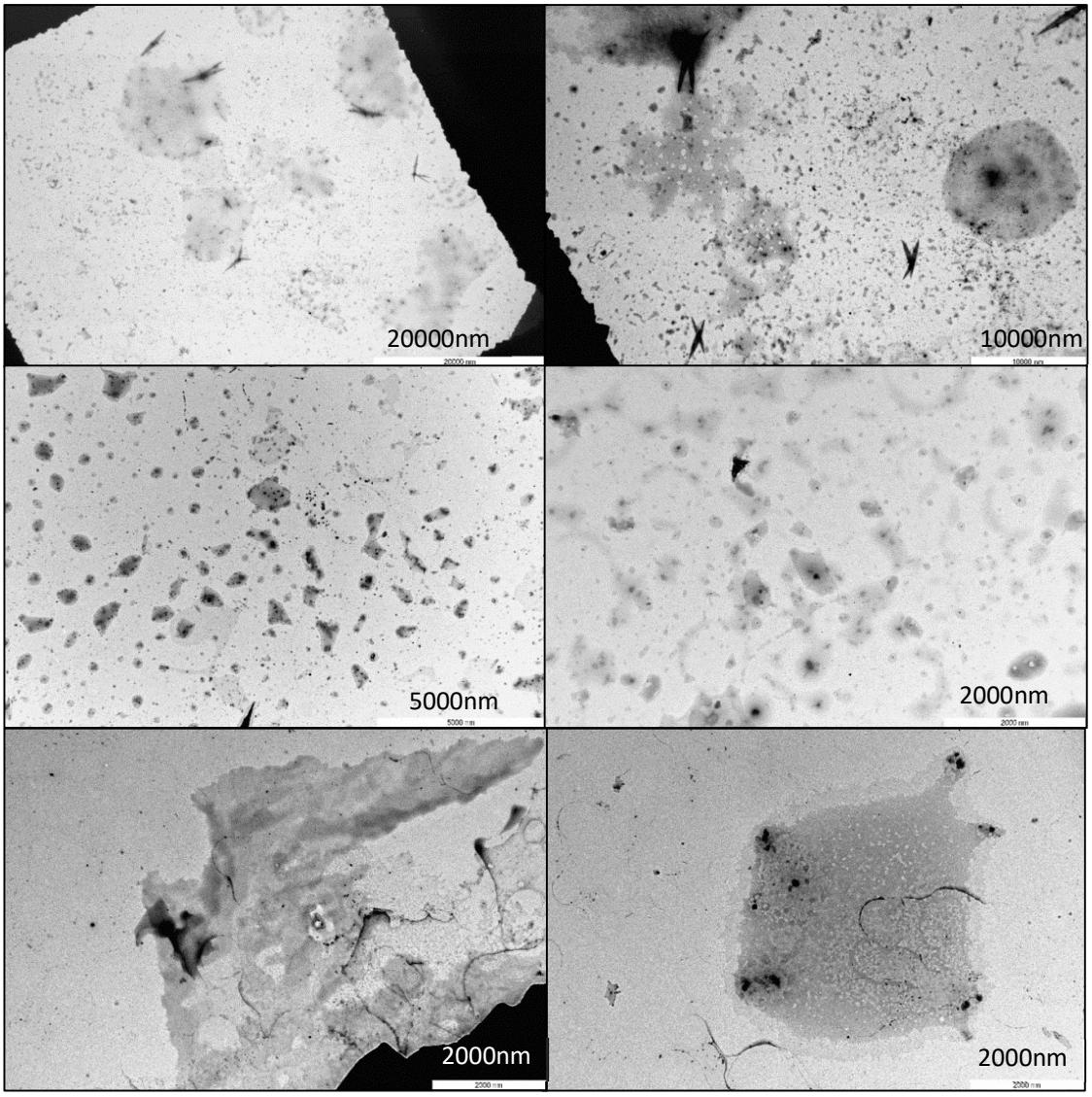


Figure 52 Images showing graphite produced from New Battery Grade Graphite processed using supercritical ethanol at 69 bar and 250 ^{o}C and fast pressure release

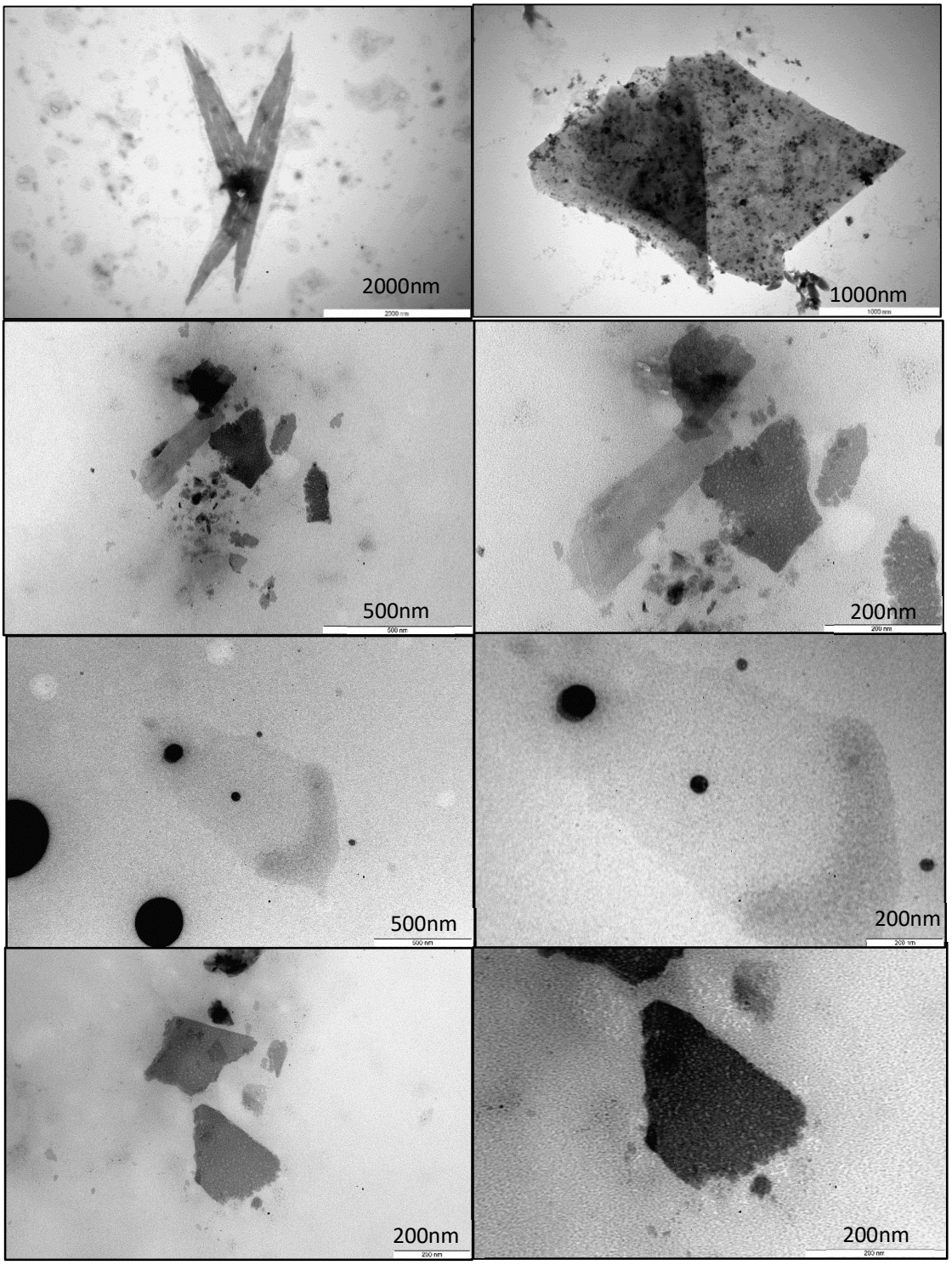


Figure 53 Images showing Graphene produced from End-of-Life Graphite processed using supercritical ethanol at 69 bar and 250 ^{o}C and fast pressure release

5.6 Continuous Separation and Upscaling

The techniques used above to produce products and recycle anode material work in the laboratory setting. The main and final product for the ReLiB project, is to produce a plant that could recycle electric car batteries for thousands of cars within the UK. The process of extracting PVDF and of upscaling graphite and therefore needs to be moved from a batch process to more of a continuous process. This could enable it to be implemented into already existing recycling plants. This means that the processes need to be simple to use and to reduce the health and safety concerns by as much as possible. The main problem with using supercritical conditions is that it expensive to get to these conditions and while at these conditions can be dangerous with high temperatures and high pressures. To limit these downsides, a need to reduce the amount of time and volume of the fluid required at these conditions. Therefore, the design of a pipe reactor system as the most efficient solution. It reduces the amount of time that the liquid spends at these dangerous conditions and an integrated transfer system is used for the heating and cooling, this would also decrease the overall energy costs for the process. A basic test design was put forward for a continuous PVDF recycle system. This can be seen in Figure 54. This design was used to outline the construction of a cheap to build small test reactor. Using pipe sizes shown in Figure 55 pipes and valves were ordered along with a furnace to be used as the heat exchanger shown in Figure 57. With the furnace being used as the heat exchanger the pipe reactor was designed to be a U-shaped, shown in Figure 56, with the middle section being removable so that anode material can be removed and replaced, without having to dismantle the pipe reactor. The thinner 1/8-inch pipe would be wrapped around the pipe reactor so that the liquid could reach supercritical conditions.

The process shown in Figure 55 is a rudimentary pipe reactor where the pump increases the pressure on the fluid so that it almost reaches critical temperature before it reaches the pipe reactor shown in Figure 57. The temperature and pressure are monitored either side of the pipe reactor so that the fluid can be kept at supercritical conditions throughout. The solvent will then have time to cool down in the cooling tank so that the PVDF drops out of suspension and can be filtered out of the fluid. The solvent is then recycled and reused.

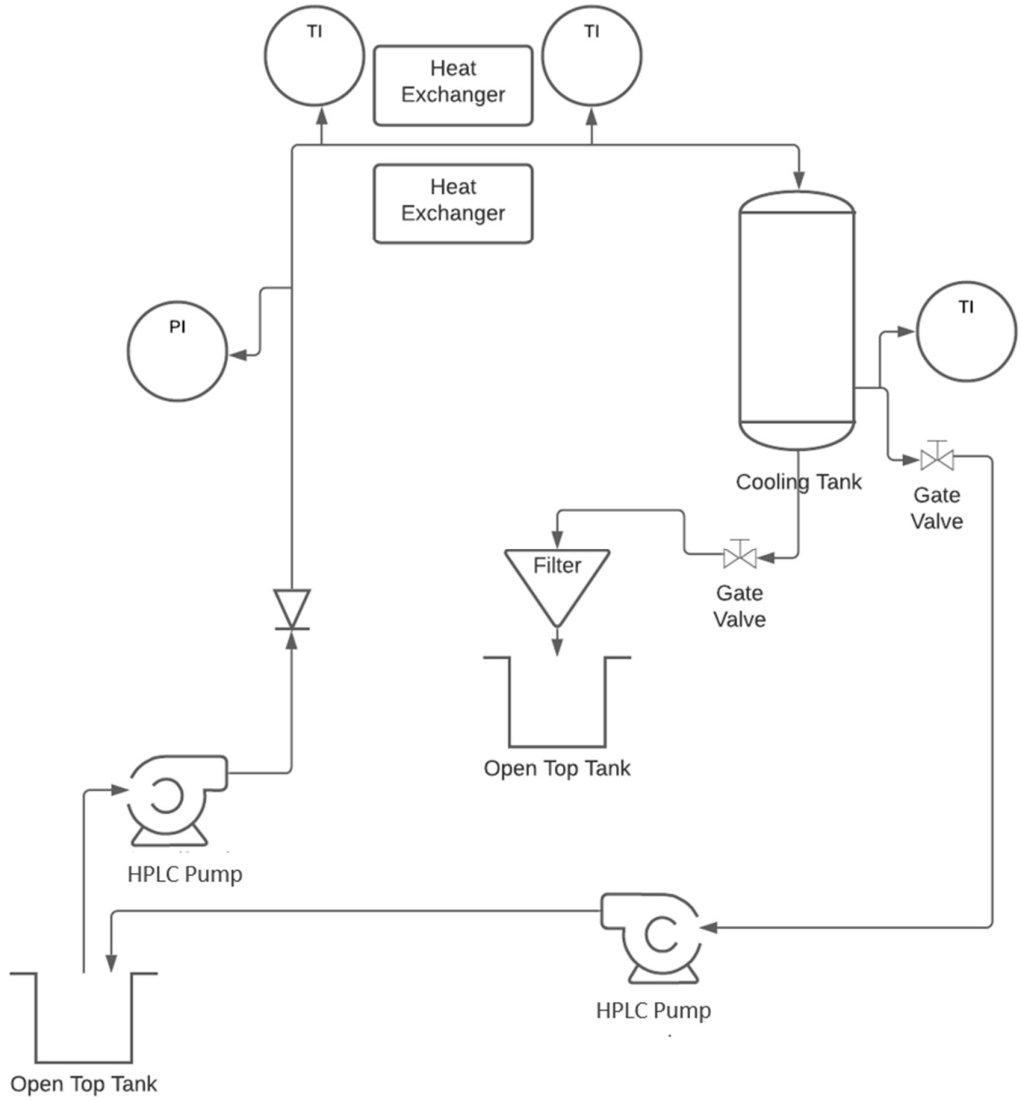


Figure 54 Flow Diagram for the Overall Continuous supercritical Extraction Process

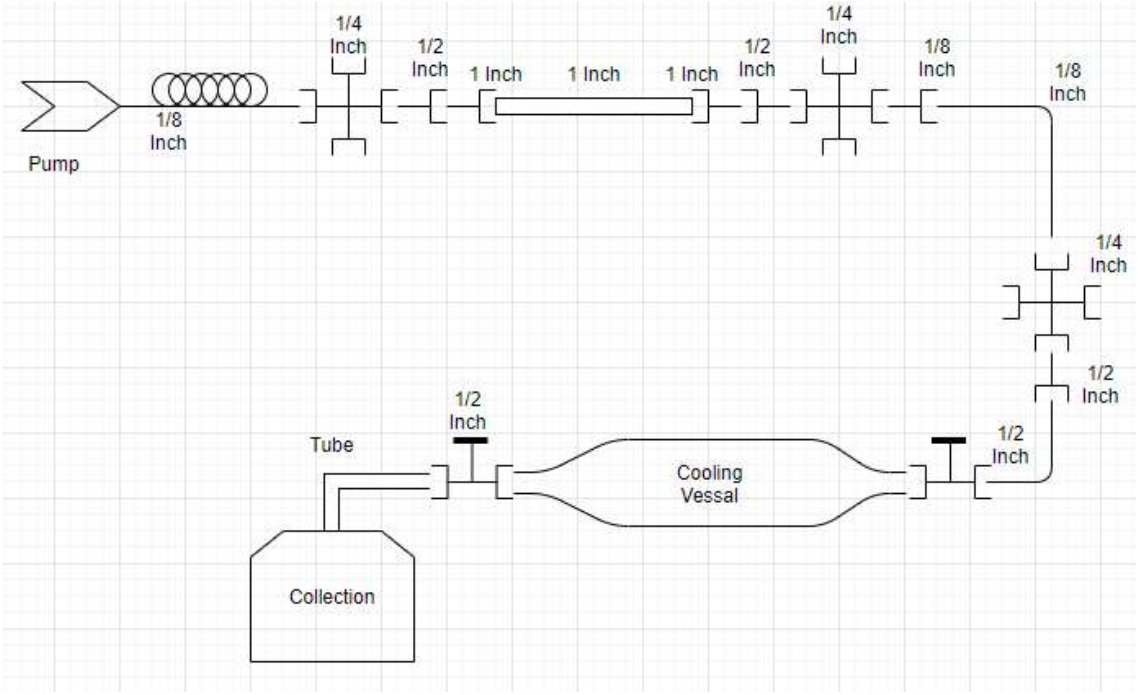


Figure 55 Diagram Showing the Pipe Reactor that could be used to Extract PVDF.

Figure 55 Diagram Showing the Pipe Reactor that could be used to Extract PVDF. Figure 56 Diagram showing the separation of the pipe reactor.is a rough design of three detachable 1-inch pipe pieces. The middle pipe would contain a metal cage which would contain the anode material stopping it from moving. The 1/8-inch pipe wraps around the entire pipe reactor so that it can all be placed inside the oven. The need for the extended wrapped pipe is to increase heat transfer to the solvent by increasing the residence time to heat the fluid and reach a critical temperature and pressure before it reaches the anode material.

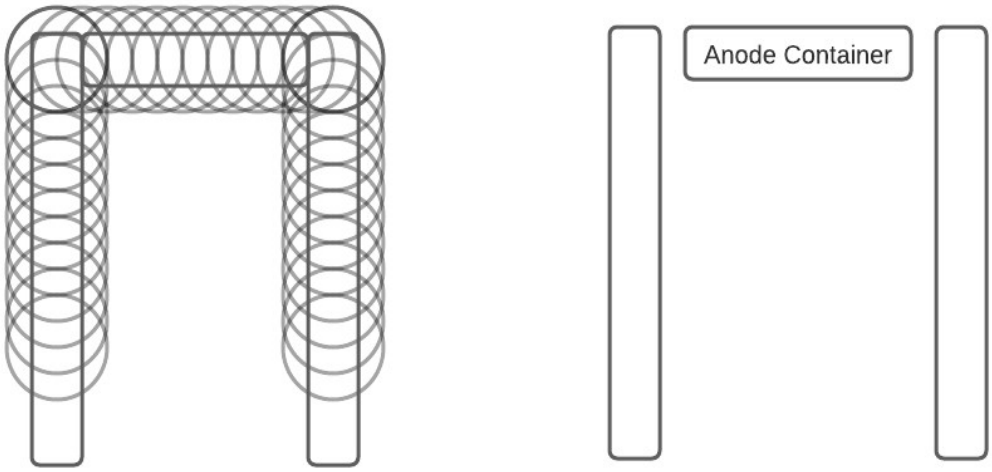


Figure 56 Diagram showing the separation of the pipe reactor.



Figure 57 The furnace that could be used for the Pipe Reactor (Carbolite Gero ELF 1100)

The process would start by pumping the liquid through the thin piping to reach supercritical pressure, the liquid would then enter the furnace to increase it to it supercritical temperature. An on/off valve would close the pipe reactor so that it could be charged with the supercritical liquid and once the

reactor was full the valve would be released creating the circuit. The liquid exiting the pipe reactor would enter a cooling vessel, the same one shown in Figure 10 that was used for the graphene production. The use of a needle valve would decrease the flow out of the cooling vessel giving enough time for the liquid to exit supercritical conditions causing the PVDF to drop out of the solution; the PVDF could then be extracted. The used ethanol would then recirculate closing the loop. Due to time restraints and Covid conditions it was not possible to be able to build this process to test the theory. If the process was built and it was successful, the upscaling of this process wouldn't require too much work. The use of multiple pipe reactors so that anode material could be re-loaded while one is undergoing supercritical extraction and one can be charged. The use of a more elaborate energy conserving heat exchanger would also be used. With the production becoming a regenerative continuous process, the production speed and operating cost will become more profitable for a production line.

6 Conclusions and Further Work

6.1 Conclusion

The extraction of PVDF was a success using supercritical solvents was examined using: TGIR, Light Microscopy and SEM.

Using IR gave the result that both the SC extraction products and the pure PVDF had the same carbon bonds; C-C, C-F and C-H. The light microscopy gave the result that with the use of methanol, ethanol and butanol, the product had a remarkably similar particle shapes and sizes. The particles produced by DCM were vastly different and will require further work to be explained as to why this is the case. It could be concluded it was the case due to the product not precipitating until the final drying stage using the vacuum pump. The SEM-EDX data gave the conclusive evidence with the products having the carbon and fluorine required for this to be PVDF. So, the extracted material was determined to be PVDF.

The contamination to the PVDF were from two sources. The oxygen can be concluded to come from the extraction process where the likelihood that under the SC conditions the PVDF underwent some oxidation, this has been decided to be because the DCM product had no oxygen contamination. The other elements contained within the PVDF products would be from the source material and manufacturing processes of the anode.

The use of acetone in this process was concluded to be less successful due to assumption that the acetone self-reacts to iso-phorone, causing a yellow-orange coloured wax to be formed dissolved within the liquid, this also discoloured the PVDF.

The production of graphene using a supercritical solvent was successful also. Two methods were used, ultra-sonic probe and rapid pressure release. Due to problems with the Sonic Probe, this method was less inconclusive and with further testing there could be merit to this process. The use of a quick built pressure release system produced successful results using both new and end-of-life graphite. The graphene produced using new graphite was thinner and decreased in concentration than when compared with the end-of-life graphite.

The design for a continuous PVDF extracting system was conceptualised and needs to be tested to see the possibility of using supercritical extraction on a larger scale. This is the next step in testing the use of supercritical fluids for the recycling of electric vehicle battery anode materials

6.2 Further Work

With complications with COVID cutting research short there are areas that can be expanded upon to further help with the recycling and production of future Li-Ion batteries. Exploring the reasons behind the extraction of PVDF, through examining the mean particle size of the products being produced.

It needs to be explored how reusable the PVDF that was extracted is in its reuse. Can it be used in the place of new pure PVDF. Will it need further refining for this to be the case. If not, then how could it be used.

The use of a continuous and regenerating system to extract battery components without the use of shredding and the production of black mass. This needs to be evaluated by producing a lab sized pilot plant to prove the concept and generate more data on the use of supercritical fluids with battery recycling.

The use of supercritical fluids on the cathode material to compare results with that of the anode material, the overall goal to recover the metal oxides without destructive methods.

Further work needs to be conducted into the production of graphene from battery graphite, with the results above showing positive results. More tests will be needed to find the quality of the graphite such as Raman. Also, a method which results in a higher production of graphene will need to be determined to make this viable.

7 References

Bai, H. *et al.* (2012) 'Preparation and characterization of poly(vinylidene fluoride) composite membranes blended with nano-crystalline cellulose', *Progress in Natural Science: Materials International*. Elsevier, 22(3), pp. 250–257. doi: 10.1016/J.PNSC.2012.04.011.

Barta, K. *et al.* (2010) 'Catalytic disassembly of an organosolv lignin via hydrogen transfer from supercritical methanol', *Green Chemistry*, 12(9), pp. 1640–1647. doi: 10.1039/c0gc00181c.

Bruce, P. G., Scrosati, B. and Tarascon, J. M. (2008) 'Nanomaterials for rechargeable lithium batteries', *Angewandte Chemie - International Edition*, pp. 2930–2946. doi: 10.1002/anie.200702505.

Budi Nursanto, E. *et al.* (2011) 'Facile synthesis of reduced graphene oxide in supercritical alcohols and its lithium storage capacity', *Green Chemistry*, 13(10), pp. 2714–2718. doi: 10.1039/c1gc15678k.

Chen, M. *et al.* (2019) 'Recycling End-of-Life Electric Vehicle Lithium-Ion Batteries', *Joule*. doi: 10.1016/j.joule.2019.09.014.

Chen, X. *et al.* (2017) 'Direct exfoliation of the anode graphite of used Li-ion batteries into few-layer graphene sheets: a green and high yield route to high-quality graphene preparation', *Journal of Materials Chemistry A*. Royal Society of Chemistry, 5(12), pp. 5880–5885. doi: 10.1039/c7ta00459a.

Dandy, L. O. *et al.* (2015) 'Accelerated degradation of Polyetheretherketone (PEEK) composite materials for recycling applications', *Polymer Degradation and Stability*. Elsevier Ltd, 112, pp. 52–62. doi: 10.1016/j.polymdegradstab.2014.12.012.

Diekmann, J. *et al.* (2017) 'Ecological Recycling of Lithium-Ion Batteries from Electric Vehicles with Focus on Mechanical Processes', *Journal of The Electrochemical Society*. The Electrochemical Society, 164(1), pp. A6184–A6191. doi: 10.1149/2.0271701jes.

Duleep, G. *et al.* (2011) 'Impacts of Electric Vehicles - Deliverable 2 Assessment of electric vehicle and battery technology', *European Comission*, (April), p. 68. Available at: http://ec.europa.eu/clima/policies/transport/vehicles/studies_en.htm%5Cnhttp://ec.europa.eu/clima/policies/transport/vehicles/docs/d2_en.pdf.

Dunn, B., Kamath, H. and Tarascon, J. M. (2011) 'Electrical energy storage for the grid: A battery of choices', *Science*, pp. 928–935. doi: 10.1126/science.1212741.

Fan, E. *et al.* (2020) 'Sustainable Recycling Technology for Li-Ion Batteries and Beyond: Challenges and Future Prospects', *Chemical Reviews*. American Chemical Society. doi: 10.1021/acs.chemrev.9b00535.

Gaines, L. (2012) 'To recycle, or not to recycle, that is the question: Insights from life-cycle analysis',

MRS Bulletin, 37(4), pp. 333–338. doi: 10.1557/mrs.2012.40.

Hadi, A. *et al.* (2016) 'Optimization of graphene production by exfoliation of graphite in supercritical ethanol: A response surface methodology approach', *The Journal of Supercritical Fluids*. Elsevier, 107, pp. 92–105. doi: 10.1016/J.SUPFLU.2015.08.022.

Harper, G. *et al.* (2019) 'Recycling lithium-ion batteries from electric vehicles', *Nature*. Nature Publishing Group, pp. 75–86. doi: 10.1038/s41586-019-1682-5.

Huang, B. *et al.* (2018) 'Recycling of lithium-ion batteries: Recent advances and perspectives', *Journal of Power Sources*. Elsevier B.V., pp. 274–286. doi: 10.1016/j.jpowsour.2018.07.116.

Huang, X. *et al.* (2014) 'Catalytic depolymerization of lignin in supercritical ethanol', *ChemSusChem*. Wiley-VCH Verlag, 7(8), pp. 2276–2288. doi: 10.1002/cssc.201402094.

Kang, D. H. P., Chen, M. and Ogunseitan, O. A. (2013) 'Potential environmental and human health impacts of rechargeable lithium batteries in electronic waste', *Environmental Science and Technology*, 47(10), pp. 5495–5503. doi: 10.1021/es400614y.

Kim, J. *et al.* (2008) 'Continuous synthesis of surface-modified metal oxide nanoparticles using supercritical methanol for highly stabilized nanofluids', *Chemistry of Materials*, 20(20), pp. 6301–6303. doi: 10.1021/cm8017314.

Marshall, J. E. *et al.* (2021) 'On the solubility and stability of polyvinylidene fluoride', *Polymers*. doi: 10.3390/polym13091354.

Melin, H. E. (2020) 'State-of-the-art in reuse and recycling of lithium-ion batteries – A research review', *Circular Energy Storage*, 1(57), pp. 1–57.

Moradi, B. and Botte, G. G. (2016) 'Recycling of graphite anodes for the next generation of lithium ion batteries', *Journal of Applied Electrochemistry*. Springer Netherlands, 46(2), pp. 123–148. doi: 10.1007/s10800-015-0914-0.

Mossali, E. *et al.* (2020) 'Lithium-ion batteries towards circular economy: A literature review of opportunities and issues of recycling treatments', *Journal of Environmental Management*, 264. doi: 10.1016/j.jenvman.2020.110500.

Nitta, N. *et al.* (2015) 'Li-ion battery materials: Present and future', *Materials Today*, pp. 252–264. doi: 10.1016/j.mattod.2014.10.040.

Okajima, I. and Sako, T. (2019) 'Recycling fiber-reinforced plastic using supercritical acetone', *Polymer Degradation and Stability*. Elsevier, 163, pp. 1–6. doi: 10.1016/j.polymdegradstab.2019.02.018.

Ramanamurty, K. V. and Salvapati, G. S. (1999) 'Catalytic cyclocondensation of acetone to isophorone', *Indian Journal of Chemistry - Section B Organic and Medicinal Chemistry*, 38(1), pp. 24–28.

Scrosati, B. and Garche, J. (2010) 'Lithium batteries: Status, prospects and future', *Journal of Power Sources*, pp. 2419–2430. doi: 10.1016/j.jpowsour.2009.11.048.

Seo, M. *et al.* (2013) 'Supercritical alcohols as solvents and reducing agents for the synthesis of reduced graphene oxide', *Carbon*. Pergamon, 64, pp. 207–218. doi: 10.1016/j.carbon.2013.07.053.

Slater, M. D. *et al.* (2013) 'Sodium-ion batteries', *Advanced Functional Materials*, 23(8), pp. 947–958. doi: 10.1002/adfm.201200691.

Song, D. *et al.* (2012) 'Recovered LiCoO2 as anode materials for Ni/Co power batteries', *Physical Chemistry Chemical Physics*, 14(1), pp. 71–75. doi: 10.1039/c1cp21936g.

Tarascon, J. M. and Armand, M. (2001) 'Issues and challenges facing rechargeable lithium batteries', *Nature*, pp. 359–367. doi: 10.1038/35104644.

Warner, G. *et al.* (2014) 'Depolymerization of organosolv lignin using doped porous metal oxides in supercritical methanol', *Bioresource Technology*. Elsevier Ltd, 161, pp. 78–83. doi: 10.1016/j.biortech.2014.02.092.

Yeo, S. Do and Kiran, E. (2005) 'Formation of polymer particles with supercritical fluids: A review', *Journal of Supercritical Fluids*, 34(3), pp. 287–308. doi: 10.1016/j.supflu.2004.10.006.

Yun, L. *et al.* (2018) 'Metallurgical and mechanical methods for recycling of lithium-ion battery pack for electric vehicles', *Resources, Conservation and Recycling*. Elsevier B.V., 136, pp. 198–208. doi: 10.1016/j.resconrec.2018.04.025.

Zhu, Y. *et al.* (2010) 'Graphene and graphene oxide: Synthesis, properties, and applications', *Advanced Materials*, 22(35), pp. 3906–3924. doi: 10.1002/adma.201001068.

Zubi, G. *et al.* (2018) 'The lithium-ion battery: State of the art and future perspectives', *Renewable and Sustainable Energy Reviews*. Elsevier Ltd, pp. 292–308. doi: 10.1016/j.rser.2018.03.002.